Weather and Climate Extremes 45 (2024) 100699

Contents lists available at ScienceDirect

Weather and Climate Extremes

journal homepage: www.elsevier.com/locate/wace

An attribution study of very intense rainfall events in Eastern Northeast Brazil

Francisco das Chagas Vasconcelos Junior [a,*], Mariam Zachariah [b], Thiago Luiz do Vale Silva [c], Edvânia Pereira dos Santos [c], Caio.A.S. Coelho [d], Lincoln M. Alves [e], Eduardo Sávio Passos Rodrigues Martins [a,r], Alexandre C. Köberle [b], Roop Singh [f], Maja Vahlberg [f], Victor Marchezini [g,h], Dorothy Heinrich [f], Lisa Thalheimer [i,j], Emmanuel Raju [k], Gerbrand Koren [l], Sjoukje Y. Philip [m], Sarah F. Kew [m], Rémy Bonnet [n], Sihan Li [o], Wenchang Yang [p], Jingru Sun [p], Gabriel Vecchi [p,q], Friederike.E.L. Otto [b]

[a] Ceará Institute for Meteorology and Water Resources, FUNCEME, Fortaleza, Brazil
[b] Grantham Institute, Imperial College London, UK
[c] Water and Climate Pernambuco Agency, APAC, Recife, Brazil, Pernambuco, Brazil
[d] Centre for Weather Forecast and Climatic Studies, National Institute for Space Research, Brazil
[e] National Institute for Space Research, Brazil
[f] Red Cross Red Crescent Climate Centre, the Netherlands
[g] Natural Hazards Center, University of Colorado at Boulder, USA
[h] National Center for Monitoring and Early Warning of Natural Hazards (Cemaden), Brazil
[i] School of Public and International Affairs, Princeton University, Princeton, USA
[j] Potsdam Institute for Climate Impact Research, Potsdam, Germany
[k] Department of Public Health, Global Health Section & Copenhagen Centre for Disaster Research, University of Copenhagen, Denmark
[l] Copernicus Institute of Sustainable Development, Utrecht University, the Netherlands
[m] Royal Netherlands Meteorological Institute (KNMI), De Bilt, the Netherlands
[n] Institut Pierre-Simon Laplace, CNRS, Sorbonne Université, Paris, France
[o] School of Geography and the Environment, University of Oxford, UK
[p] Department of Geosciences, Princeton University, Princeton, USA
[q] High Meadows Environmental Institute, Princeton University, Princeton, NJ, USA
[r] Graduate Program in (Civil Engineering, Water Resources, Environmental Sanitation, and Geotechnics), Federal University of Ceará, Fortaleza, CE, Brazil

ABSTRACT

Severe floods and landslides in Eastern Northeast Brazil in May 2022 led to severe impacts with human losses and material damage. These disasters were a direct consequence of extremely heavy rainfall days. A rapid attribution study was performed to assess the role of anthropogenic climate change in 7 and 15-day mean rainfall over this region. A dense network of 389 weather stations was analysed resulting in 79 selected stations containing consistent and spatially well-distributed data over the study region with records starting in the 1970s. Daily rainfall from a multi-model ensemble of climate simulations were also examined to investigate the role of climate change in modifying the likelihood of such extreme events over the studied region. However, such an analysis was hindered by the fact that most investigated models have deficiencies in representing convection associated with warm rains, which are key for the manifestation of such extreme events associated with Easterly Wave Disturbances. From the observational analysis, both 7 and 15-day mean events in 2022 were found to be exceptionally rare, with an approximately 1-in-500 and 1-in-1000 chance of happening in any year in today's climate, respectively. Even though both events were located far outside the previously observed records, because of the short observational record and associated uncertainties it was not possible to quantify how much climate change made these events more likely to happen. The performed analysis also revealed that global warming increased the intensity of such extreme rainfall: rainfall events as rare as those investigated here occurring in a 1.2 °C cooler climate would have been approximately a fifth less intense. Combining observations with the physical understanding of the climate system, this study showed that human-induced climate change is, at least in part, responsible for the increase in likelihood and intensity of heavy rainfall events as observed in May 2022. Besides, the extreme nature, as a result of such events, made it so extraordinary that population exposure and vulnerability was identified as the main driver for the observed impacts, although long-term impacts and recovery will likely be mediated by socio-economic, demographic and governance factors.

* Corresponding author.
E-mail address: francisco.vasconcelos@funceme.br (F.C. Vasconcelos Junior).

https://doi.org/10.1016/j.wace.2024.100699
Received 19 January 2023; Received in revised form 8 March 2024; Accepted 27 May 2024
Available online 28 May 2024
2212-0947/© 2024 Published by Elsevier B.V. This is an open access article under the CC BY-NC-ND license (http://creativecommons.org/licenses/by-nc-nd/4.0/).

1. Introduction

The combination of high spatial and temporal rainfall variability and the highest proportion of people living in poverty in Brazil makes the Northeast of Brazil (NEB) particularly vulnerable to climate variability and change impacts on extremes events (Magalhães, 1996; Marengo et al., 2019). Furthermore, there is strong evidence that climate change will increase drought risk and severity in this region (IPCC, 2021[1]). Although the NEB has historically been known for extreme droughts, heavy rainfall events also have a history of severely impacting the area (Ribot et al., 1996; Marengo et al., 2017). In the week beginning on May 23rd, 2022, very heavy rainfall started falling over eastern of NEB, in the states of Pernambuco, Alagoas, Paraíba, Sergipe and Rio Grande do Norte (Fig. 1). The rainfall began to intensify on the 25th of May, leading to flash floods and landslides in NEB and a dam break in the state of Paraíba (FloodList, 26 May 2, 022[2]). In less than 24 h on May 27–28, parts of Pernambuco received about 70% of the total rainfall expected for the entire month of May. Fig. 2 shows this event, averaged over the week when most of the associated impacts were reported (Fig. 2(a)) and over the fortnight when the precipitation was high (Fig. 2(b)). Fig. 2(c) depicts the Easterly Disturbance Wave peak in terms of circulation, humidity and vertical velocity at low level of the troposphere which was the main actor in the event (Vale Silva et al., 2023) (see Table 6).

This heavy rainfall event triggered extensive landslides and widespread floods in the affected areas, resulting in 133 fatalities and over 25,000 people displaced, predominantly impacting residents of low-income neighbourhoods near hillsides (Gizmodo, 1 June 2, 022[3]). Following the disaster, at least 80 municipalities across Pernambuco and Alagoas declared a state of emergency (Civil Defense *Pernambuco*, 2022; Civil Defense *Alagoas*, 2022). The Metropolitan Region of Recife (RMR) in the state of Pernambuco was severely impacted by this hazard event - one of the worst extreme rainfall events in its history.

Easterly disturb waves, that are typical meteorological events for this season, have the potential to cause heavy and widespread rainfall as well as thunderstorms, and were the primary driver of this hazard event in May 2022 (Vale Silva et al., 2023). Due to the location's topography, characterized by low altitudes, the urban drainage system is highly susceptible to the effects of the tides (Silva et al., 2017). In this context, the impacts derived from intense rainfall in this region, notably flooding, are recognized for their accentuation during periods of rising tides (Marengo et al., 2023). However, with the rise in sea level in the Recife area (Harari et al., 2004), an increase in the propensity to flooding in the city is projected, especially in situations involving intense rainfall and high tides, in a scenario of rising sea levels (Costa et al., 2010). However, the impacts of the May 2022 event were largely ascribed to the precipitation itself.

In this study, we analyse precipitation over a small region enclosing the area with the highest impacts. Recognising the localised nature of the rainfall, for this analysis, we restrict ourselves to using only high-resolution climate models (≤60 km). However, the resolution of these models is still such that very few grid boxes represent the coastal region, with the largest impacts. In order to be able to use these models and compare with observations, we choose to extend the region slightly further inland. The chosen spatial definition is a rectangular domain defined by 10°S-5°S; 36°W-34.5°W, in which we use land points only in the black box in Fig. 2. Consideration is also given to the homogeneity of the region (Fig. 3(a)). The study box is dominated by one type of climate zone - the tropical Savanna (Fig. 3(b)) and lies to the east of a drier region in climatological precipitation (Fig. 3(c)). Because the maximum impacts were witnessed in one week, we use as a temporal definition the annual maximum 7-day average precipitation, RX7d. Because the event is furthermore characterised by higher-than-average precipitation over periods longer than a week, with several peaks, we also use the alternative temporal definition of the annual maximum of 15-day average precipitation, RX15d.

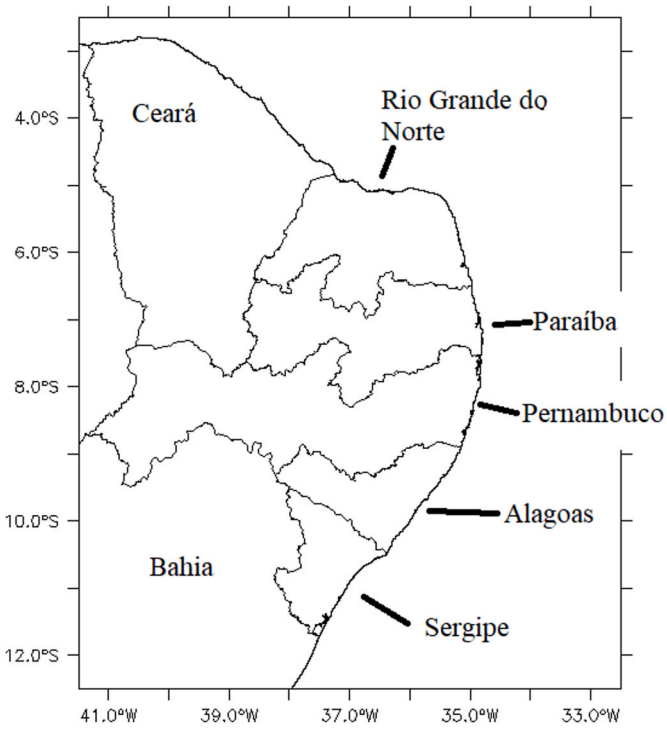

Fig. 1. Eastern of Northeast Brazil region.

The period from March to August is the rainy season of the eastern Northeast coast of Brazil. Generally, in March and April the Intertropical Convergence Zone (ITCZ) has its largest incursion to the Southern Hemisphere and in its seasonal march produces rainfall events throughout the over the Northeast Brazil region through deep convection and the so-called cold rain (Waliser and Jiang, 2015; Grimm 2011). On the other hand, the rainfall over the eastern coast of Northeast Brazil is largely produced by easterly wave disturbances (Gomes et al., 2015). Even though these waves occur all year round, they have a peak activity during the months from May to August, reaching the coast with heavy rain and with rainfall events lasting for a few days. They have a local-regional spatial scale of local-regional action and very often are associated with warm convective rainfall (Liu and Zipser, 2009). These characteristics are hard to be represented in climate models due to the lack of high spatial resolution and adequate convection schemes. Expressive daily rainfall amounts over 150 mm are commonly recorded in this region and are usually associated with easterly wave disturbances (Gomes et al., 2015). For example, from 21-May until 01-Jun 2017, some cities in Pernambuco experienced consecutives days with very high daily rainfall records, with the 7-day event in Sirinhaém, Rio Formoso and Ribeirão stations recorded 591, 569.3 and 468.5 mm, respectively. Other recent extreme rainfall events that were also associated with severe impacts in Pernambuco include those recorded in the years 2000, 2004, 2005, 2010, 2011, 2017, 2019 and 2021.

So far, not many attribution studies for floods or extreme precipitation events have been carried out for regions in Northeast Brazil (Martins et al., 2017). One recent study by Rudorff et al. (2021) has assessed river floods from the Parnaíba river, situated in a different climate zone to the west of our study region, that occurred in the year 2018, 2019 and 2022. The authors found that anthropogenic factors have increased the

[1] https://www.ipcc.ch/report/ar6/wg1/downloads/factsheets/IPCC_AR6_WGI_Regional_Fact_Sheet_Central_and_South_America.pdf.

[2] https://floodlist.com/america/brazil-floods-pernambuco-alagoas-paraiba-may-2022#.

[3] https://gizmodo.com/brazil-landslides-recife-pernambuco-floods-1848997858.

likelihood of these events by approximately 30%, although the link to observed (decreasing) trends is not clear. This study contributes to enrich the literature on this scope by performing an attribution analysis for the May 2022 extreme precipitation events over Eastern Northeast Brazil aiming to identify the possible anthropogenic-driven climate factors behind the observed impacts.

2. Data and methods

2.1. Observational data

2.1.1. Station data

We analysed long-term observed daily precipitation records from 1960-present, from 389 weather stations spread over our study region,

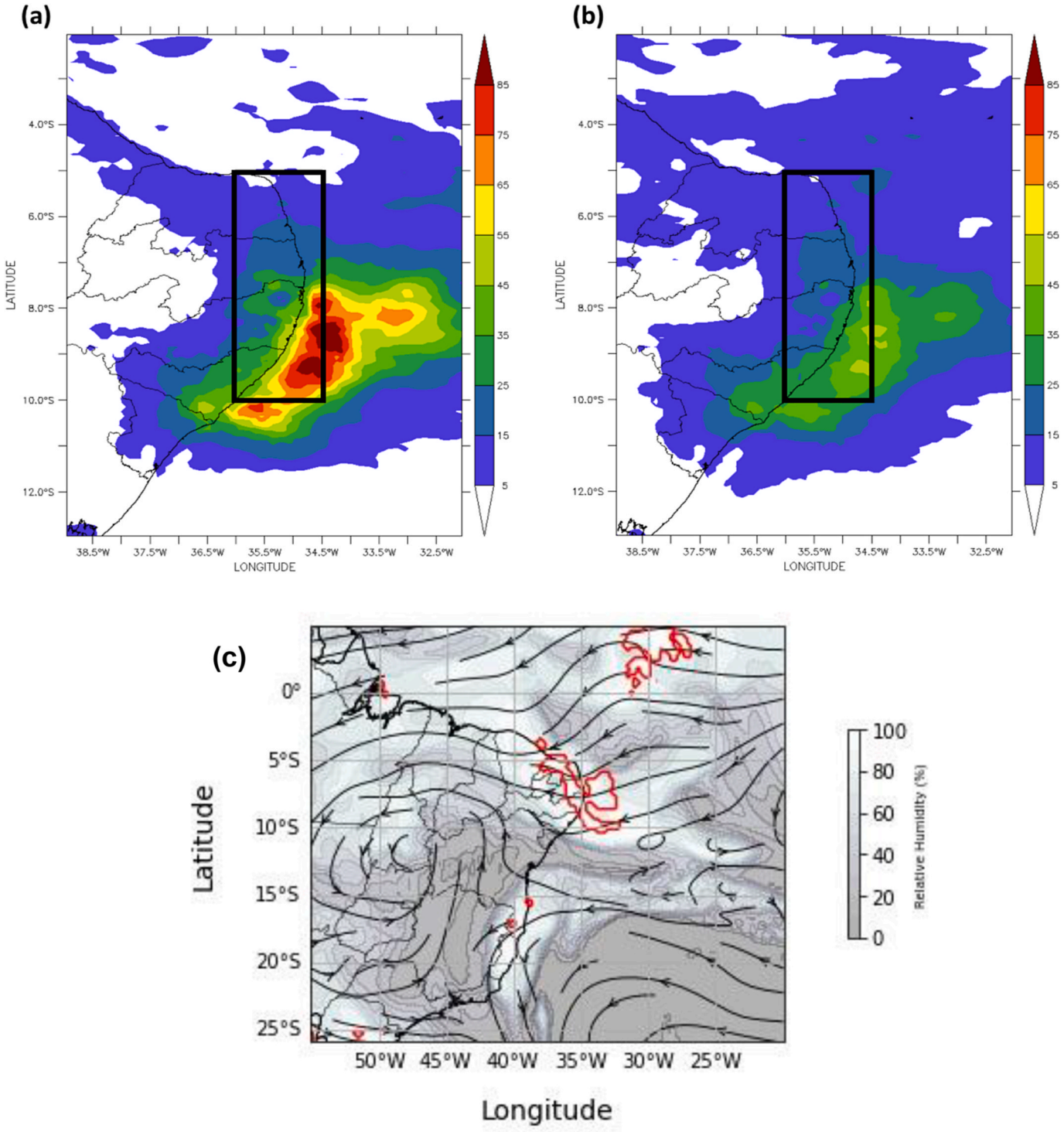

Fig. 2. (a) Observed average 7-day rainfall for 25–31 May 2022 and (b) 15 -day rainfall for 25 May-8 June 2022, over North Eastern Brazil from MERGE-GPM dataset. The colorbar is in the unit mm/day. (c) Streamlines, relative humidity (shaded) and omega (contours) at 700 hPa on May 28, 2022 00 UTC, the red solid curve depicts omega less than −1 Pa/s. (For interpretation of the references to color in this figure legend, the reader is referred to the Web version of this article.)

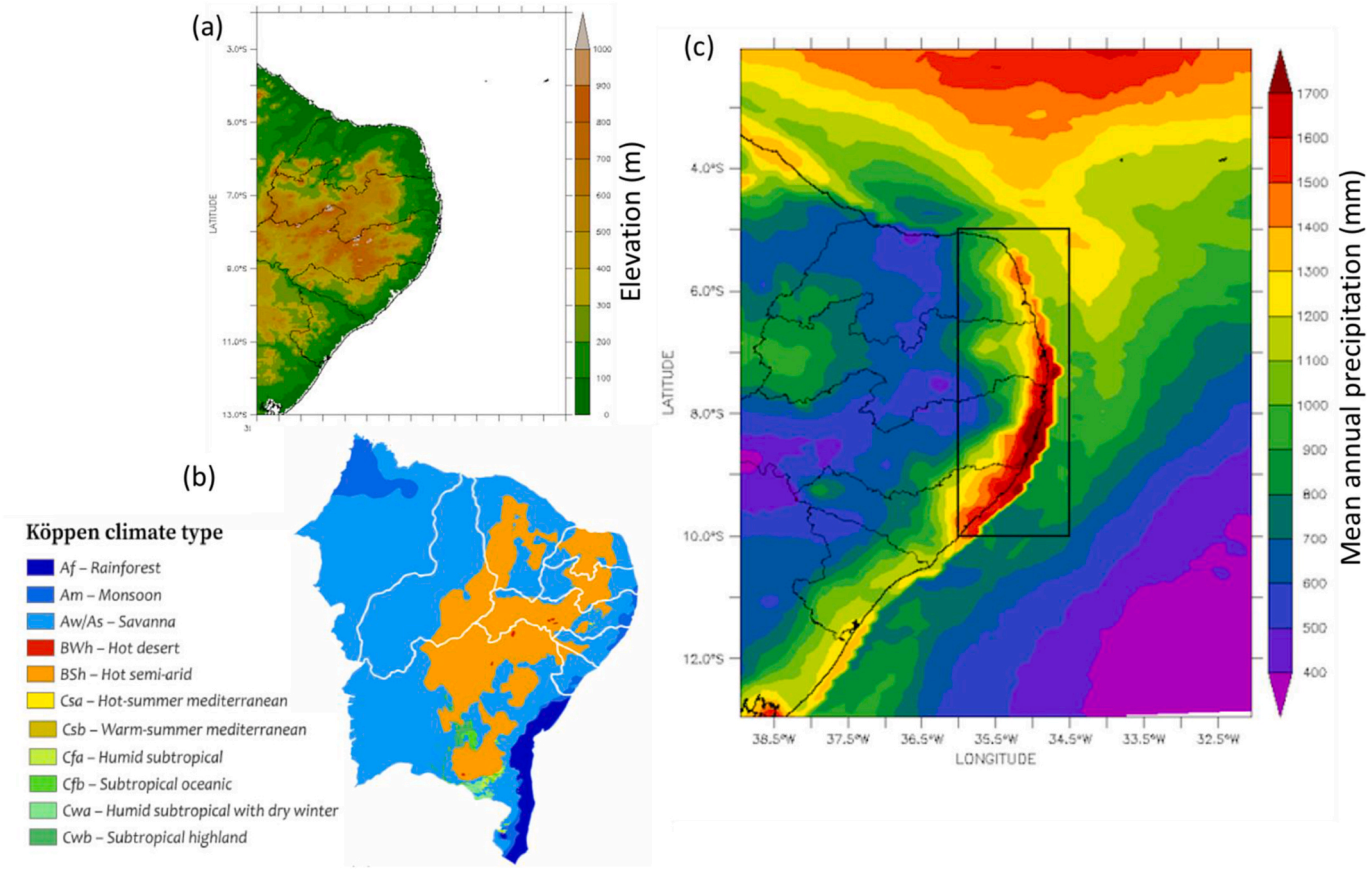

Fig. 3. (a) Topography of the region, with ocean displayed as white area and state borders indicated by black lines. (b) Köppen Climate Zones in Northeast Brazil (Alvares et al., 2013). (c) Annual mean precipitation (mm) over Northeast Brazil from MERGE-GPM dataset (Rozante et al., 2010). The study region is indicated by the black box.

as shown in Fig. 4(a). The network is sparse in the beginning of the time series, and becoming denser from the 80's. These stations are owned and monitored by the meteorology/hydrology state service institutions in the states of Rio Grande do Norte, Paraíba, Pernambuco and Alagoas (Rio Grande do Norte Agricultural Research Institute - EMPARN,[4] Water Management Executive Agency – AESA,[5] Climate and Water Pernambuco Agency[6] - APAC and State Environmental and Water Resources Secretariat[7] - SEMARH) and federal institutions (National Institute of Meteorology - INMET[8] and National Water and Sanitation Agency - ANA[9]).

The time series of these 389 stations have been averaged to represent the average precipitation over the area (Fig. 4(a)). However, to avoid spurious trends due to inhomogeneity in the number of stations available in time, we also averaged over the 75 stations that have data from at least from 1970 until May 2022, and over the 11 stations with data from 1960 until now (a subset of the 75 stations). The distribution of the 75 station locations is approximately uniformly spaced (Fig. 4(b)), whereas the 11 stations with the longest data are concentrated over a small region (Fig. 4(c)).

We compare the annual 7-day maxima and annual 15-day maxima of the three different station averages with ERA5 data (Hersbach et al., 2020) and GPM-Merge (Rozante et al., 2010) averaged over the study area (see Fig. 5). The GPM-Merge dataset is only used for this comparison, as it is too short for an extreme value analysis. The ERA5 data differs from the other time series and is therefore considered to be less reliable for this specific region. The 75 stations average resembles the average over 389 stations well over most of the years and results between the 389 stations average and the 75 stations average are consistent in terms of data valid and values (not shown). The 11 stations average diverges from the other time series. This may have to do with the unequal distribution of these stations across the region, being located in a small subregion of the full rectangular study area. Therefore the 11 stations average is not considered for further analysis. We thus continue the analysis of observations with the 75 stations average (Fig. 5).

As a measure of anthropogenic climate change, we use the (low-pass filtered with a 4-year moving average) global mean surface temperature (GMST), where GMST is taken from the National Aeronautics and Space Administration/Goddard Institute for Space Science (NASA/GISS) surface temperature analysis (GISTEMP, Hansen et al., 2010; Lenssen et al., 2019).

2.2. Model and experiment descriptions

We use three different multi-model ensembles from climate modelling experiments using very different framings (Philip et al., 2020): Sea surface temperature (SST) driven global circulation high resolution models, coupled global circulation models and regional climate models.

The first set of models used in the analysis include the AM2.5C360 (Yang et al., 2021; Chan et al., 2021) and the FLOR (Vecchi et al., 2014) climate models developed at Geophysical Fluid Dynamics Laboratory (GFDL). The AM2.5C360 is an atmospheric GCM based on that in the

[4] www.emparn.rn.gov.br.
[5] http://www.aesa.pb.gov.br.
[6] https://www.apac.pe.gov.br.
[7] http://www.semarh.al.gov.br.
[8] https://portal.inmet.gov.br.
[9] https://www.gov.br/ana/en.

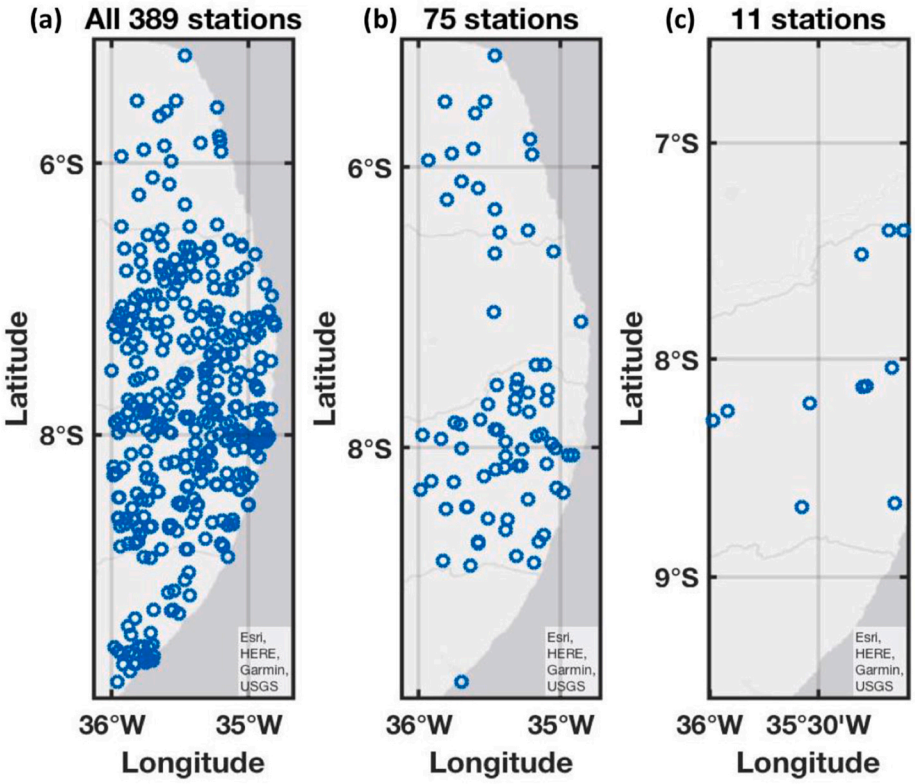

Fig. 4. Locations of weather stations within the study region. (a) All 389 stations (b) 75 stations with data from at least 1970. (c) 11 stations with data since 1960 (subset of 75 stations in panel (b)).

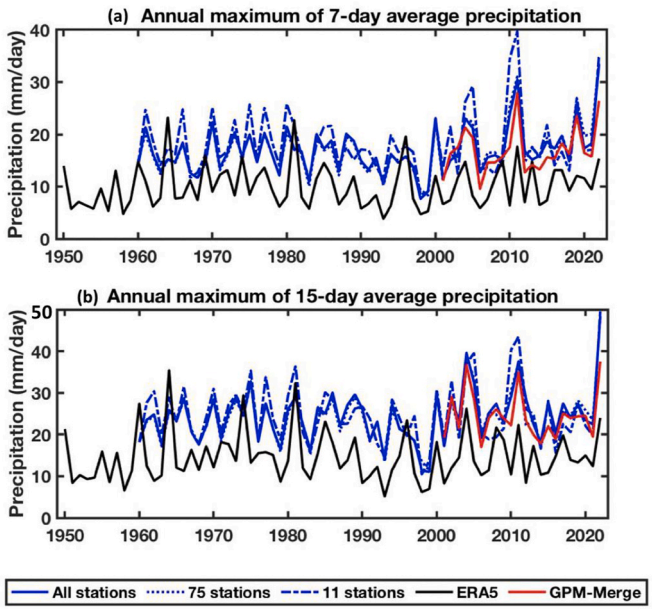

Fig. 5. (a) Time series of annual 7-day maximum precipitation in [mm/day] and (b) 15-day maximum precipitation in [mm/day] for different selections of stations (all, 75 or 11) and two different observations/reanalyses (ERA5, GPM-Merge).

FLOR model (Delworth et al., 2012; Vecchi et al., 2014) with a horizontal resolution of 25 km. Ten ensemble simulations of the Atmospheric Model Intercomparison Project (AMIP) experiment (1871–2020) are analysed. These simulations are initialised from ten different pre-industrial conditions but forced by the same SSTs from HadISST1 (Rayner et al., 2003) after groupwise adjustments (Chan et al., 2021), as well as the same historical radiative forcings. The FLOR model, on the other hand, is an atmosphere-ocean coupled GCM with a resolution of 50 km for land and atmosphere and 1° for ocean and ice. Five ensemble simulations from FLOR are analysed, which cover the period from 1860 to 2100 and include both the historical and RCP4.5 experiments driven by transient radiative forcings from CMIP5 (Taylor et al., 2012).

The second ensemble is the HighResMIP SST-forced model ensemble (Haarsma et al., 2016), the simulations for which span from 1950 to 2050. The SST and sea ice forcings for the period 1950–2014 are obtained from the 0.25° x 0.25° Hadley Centre Global Sea Ice and Sea Surface Temperature dataset that are area-weighted re-gridded to match the climate model resolution (see Table 1). For the 'future' time period (2015–2050), SST/sea-ice data are derived from RCP8.5 (CMIP5) data and combined with greenhouse gas forcings from SSP5-8.5 (CMIP6) simulations (see Section 3.3 of Haarsma et al., 2016 for further details).

The third ensemble is the Coordinated Regional Climate Downscaling Experiment CORDEX-CORE (10 models with at 0.44° resolution (SAM-44) and 4 models at 0.22° resolution (SAM-22)) multi-model ensemble (Gutowski et al., 2016; Giorgi et al., 2021), comprising 14 simulations resulting from pairings of Global Climate Models (GCMs) and Regional Climate Models (RCMs) (see Table 2 below). These simulations are composed of historical simulations up to 2005 and extended to the year 2100 using the RCP8.5 scenario (see Tables 3, 4, 5 and 6).

For model validation the years 1960–2022 have been used (1970–2022 for the SAM-22 models), which is the period for which the observed data is available. For the model analysis all data up to 2022 has been used. Because of model deficiencies we do not include the years after 2022 for a projection into the future (see section 4).

2.3. Statistical methods

In this study we analyse precipitation time series from eastern coast

Table 1
List of HighResMIP models used in the study.

Model	Resolution	Institute
CNRM-CM6-1-HR	~50 km	Centre National de Recherches Météorologiques
EC-Earth3P-HR	~40 km	EC-Earth-Consortium
HadGEM3-GC31-HM	~25 km	UK Met Office, Hadley Centre
HadGEM3-GC31-MM	~60 km	UK Met Office, Hadley Centre

of Northeast Brazil (on the box depicted in Fig. 2(a)) for 7-day and 15-day annual maxima where long records of observed data are available. Methods for observational and model analysis and for model evaluation and synthesis are used according to the World Weather Attribution Protocol, described in Philip et al. (2020), with supporting details found in van Oldenborgh et al. (2021) and Ciavarella et al. (2021).

The analysis steps include: (i) trend calculation from observations; (ii) model validation; (iii) multimethod multi-model attribution of the event with return period of 'n' years (estimated from observations in step (i)) and (iv) synthesis of the attribution statement. From observed data, we first calculate the return periods, Probability Ratio (PR) and change in intensity of the event under study for comparing between the current climate proxied by the observed GMST value of 2022 and a past climate that would have been before humans started warming the planet, when GMST (1850–1900, based on the Global Warming Index https://www.globalwarmingindex.org) was cooler by 1.2 °C, as follows. To statistically model the event under study, we use a Generalised Extreme Value (GEV) that scales with GMST:

$$F(p) = exp\left[-\left(1 + \xi\frac{p-\mu}{\sigma}\right)^{\frac{1}{\xi}} \right]$$

$$\mu = \mu_0\, exp\left(\frac{\alpha T'}{\mu_0}\right),$$

$$\sigma = \sigma_0\, exp\left(\frac{\alpha T'}{\mu_0}\right),$$

with p precipitation, T' the GMST anomaly, μ the location parameter, σ the scale parameter and ξ the shape parameter and α the trend that is fitted together with μ_0 and σ_0. In the fit, both the dispersion parameter (the ratio of the scale and location parameter) and the shape parameter are constant. The PR is calculated as the probability of occurrence (return period) of an event of the same (or larger) magnitude as observed in the current climate, divided by the probability of occurrence of the same event in the climate of the past. In the GEV analysis, the confidence intervals are estimated using a non-parametric bootstrap. The uncertainty ranges obtained from the bootstrap procedure provide information on whether the trend is outside the range of deviations expected by natural variability. We repeat the above steps for the annual maxima series estimated from the climate model simulations, to get PR and intensity changes of the respective events of return period 'n' years (estimated from observations) between the current 2022 climate and a climate that would have been 1.2 °C cooler. Next, results from observations and models that pass the validation tests are synthesised into a single attribution statement, following the methodology described in Philip et al. (2020), Ciavarella et al. (2021) and Li & Otto (2022).

Table 2
List of regional climate models used with their driving global climate models (see Gutowski et al., 2016 for a description of the Cordex experiment and Taylor et al. (2012) for a description of the GCMs).

Regional Climate Model	Resolution	Global Climate Model	Period
REMO2015	0.22°	MPI-ESM-LR	11970–2100
REMO2015	0.22°	NorESM1-M	11970–2100
RegCM4-7	0.22°	MPI-ESM-MR	11970–2099
RegCM4-7	0.22°	NorESM1-M	11970–2099
REMO2009	0.44°	MPI-ESM-LR	11950–2100
SMHI-RCA4	0.44°	CSIRO-Mk3-6-0	11951–2100
SMHI-RCA4	0.44°	EC-EARTH	11951–2100
SMHI-RCA4	0.44°	IPSL-CM5A-MR	11951–2099
SMHI-RCA4-7	0.44°	MIROC5	11951–2099
SMHI-RCA4	0.44°	HadGEM2-ES	11951–2100
SMHI-RCA4	0.44°	MPI-ESM-LR	11951–2100
SMHI-RCA4	0.44°	NorESM1-M	11951–2100
SMHI-RCA4	0.44°	GFDL-ESM2M	11951–2100
UCAN_WRF341I	0.44°	CanESM2	11950–2100

3. Observational analysis: return time and trend

3.1. Analysis of point station data

Fig. 6(a–b) shows the time series of the station-averaged annual 7-day and 15-day maximum precipitation including the 10-year running mean. The increasing trend in the amount of rainfall associated with these accumulations is consistent with previous studies that report increase in rainfall in the Northeast Brazilian coast in recent years as compared to the past (Caravalho et al., 2020). The magnitudes of the May 2022 event- 33.96 mm/day for the 7-day event and 23.95 mm/day for the 15-day event, are the highest in the respective records, as can be seen in these figures (last data points in the time series).

Fig. 7(a) shows the response of annual maximum 7-day average precipitation to the global mean surface temperature, while Fig. 7(b) shows the return period curve of the 7-day event in the current climate and in the past climate when the global mean temperature was 1.2 °C cooler. The return period of such an event in the current climate is 500 years (95% Confidence Interval (CI) 66 years to ∞). The positive trend in panel (a) indicates a tendency towards more and heavier precipitation events in recent years. The probability ratio is 43000 (95% CI 1.7 to ∞) and equivalently, the intensity change is 27% (95% CI 0.95%–59%). Fig. 7(c–d) shows the trends and the GEV-fits based on the 15-day event definition. The return period in this case is found to tend to ∞ (lower bound of 240,000 years), which implies that a 15-day event of this magnitude is very extreme even for the current climate which is 1.2 °C warmer than pre-industrial. Consequently, the probability ratio also cannot be defined. The intensity change ranges from 16 to 38.5% (at 95%CI) with a best estimate of 13%.

For ascertaining that there are no inconsistencies in the results arising from (i) the choice of the subset of 75 representative stations (Fig. 4(b)) instead of all 389 stations (Fig. 4(a)) for reasons explained in Section 2.1, and (ii) the choice of time series to include the 1960–1969 period when the stations were sparse and concentrated to a smaller region as shown in Fig. 4(c)), we repeat the above analysis for the 7-day and 15-day events, for two additional cases:

1. Considering all 389 stations for 1960–2022 (plots shown in Fig. S5).
2. Considering 75 stations for 1970–2022 (plots shown in Fig. S6).

We find that there is no indication of differences in the estimates for return period of the 2022 event, probability ratio and change in intensity between any of these cases.

3.2. Influence of modes of natural variability

During the period of heavy precipitation and the preceding months there has been an ongoing La Niña event (Jones, 2022). This modulates the rainfall variability over Northeast Brazil, and it may have exacerbated the average rainfall in the eastern Northeast Brazil (ENEB). Fig. 8 shows the correlations between the combined GPCC v2020 + monitoring product V6 + first guess (Schneider et al., 2020; Ziese et al., 2011) and the NCDCv5 ERSST Sea Surface Temperature (SST) values (Huang et al., 2017). SST values in the Southern Atlantic Ocean were only

Table 3
Evaluation results for the climate models considered for the attribution analysis of annual maximum 7-day rainfall in the year 2022, over the study region. The table contains qualitative assessments of seasonal cycle and spatial pattern of precipitation from the models (good, reasonable, bad) along with estimates for dispersion parameter, shape parameter and event magnitude. The corresponding estimates for observations are shown in blue. Based on overall suitability, the models are classified as good, reasonable and bad, shown by green, yellow and red highlights, respectively.

Observations	Seasonal cycle	Spatial pattern	Dispersion	Shape parameter	Event magnitude (mm/day)
Station			0.243 (0.187 ... 0.293)	-0.14 (-0.43 ... 0.019)	33.95
Model					**Threshold for 500-yr return period (mm/day)**
FLOR historical-rcp45 (5)	reasonable	Good	0.272 (0.248 ... 0.292)	-0.049 (-0.12 ... 0.017)	45.188
CNRM-CM6-1-HR HighResMIP (1)	good	Good	0.190 (0.157 ... 0.215)	-0.042 (-0.21 ... 0.10)	27.773
EC-Earth3P-HR HighResMIP (1)	reasonable	Good	0.298 (0.230 ... 0.347)	0.046 (-0.15 ... 0.21)	19.848
HadGEM3-GC31-HM HighResMIP (1)	reasonable	reasonable	0.265 (0.199 ... 0.311)	-0.12 (-0.29 ... 0.066)	38.075
HadGEM3-GC31-MM HighResMIP (1)	reasonable	reasonable	0.306 (0.245 ... 0.355)	0.088 (-0.10 ... 0.21)	45.157
AM2.5C360 AMIP (10)	reasonable	Good	0.291 (0.274 ... 0.313)	-0.042 (-0.12 ... 0.011)	47.952
MPI-ESM-LR / REMO2015 CORDEX SAM-22 (1)	bad	Bad	0.161 (0.115 ... 0.191)	-0.13 (-0.46 ... 0.089)	33.551
NorESM1-M / REMO2015 CORDEX SAM-22 (1)	reasonable	reasonable	0.230 (0.179 ... 0.269)	0.027 (-0.34 ... 0.23)	29.41
MPI-ESM-MR / RegCM4-7 CORDEX SAM-22 (1)	bad	Bad	0.428 (0.333 ... 0.489)	0.35 (0.079 ... 0.73)	233.28
NorESM1-M / RegCM4-7 CORDEX SAM-22 (1)	reasonable	reasonable	0.568 (0.442 ... 0.662)	-0.29 (-0.70 ... 0.059)	79.042
MPI-ESM-LR / REMO2009 CORDEX SAM-44 (1)	bad	Bad	0.145 (0.114 ... 0.171)	0.028 (-0.15 ... 0.19)	41.279
CSIRO-Mk3-6-0 / SMHI-RCA4 CORDEX SAM-44 (1)	bad	Bad	0.120 (0.0950 ... 0.139)	-0.0020 (-0.23 ... 0.23)	11.452
EC-EARTH / SMHI-RCA4 CORDEX SAM-44 (1)	bad	Bad	0.176 (0.128 ... 0.205)	0.24 (0.026 ... 0.49)	67.528
IPSL-CM5A-MR/ SMHI-RCA5 CORDEX SAM-44 (1)	reasonable	Bad	0.262 (0.204 ... 0.308)	-0.14 (-0.34 ... 0.016)	50.407
MIROC5/ SMHI-RCA4 CORDEX SAM-44 (1)	reasonable	reasonable	0.335 (0.268 ... 0.387)	0.045 (-0.17 ... 0.24)	58.86
HadGEM2-ES / SMHI-RCA4 CORDEX SAM-44 (1)	reasonable	reasonable	0.313 (0.236 ... 0.378)	-0.36 (-0.54 ... -0.24)	37.861
MPI-ESM-LR / SMHI-RCA4 CORDEX SAM-44 (1)	bad	Bad	0.202 (0.154 ... 0.236)	-0.078 (-0.29 ... 0.11)	40.587
NorESM1-M / SMHI-RCA4 CORDEX SAM-44 (1)	reasonable	reasonable	0.383 (0.301 ... 0.442)	-0.13 (-0.34 ... 0.021)	43.636
GFDL-ESM2M / SMHI-RCA4 CORDEX SAM-44 (1)	bad	Bad	0.294 (0.223 ... 0.351)	0.24 (-0.10 ... 0.58)	117.06
CanESM2/ UCAN_WRF341I CORDEX SAM-44 (1)	reasonable	reasonable	0.393 (0.300 ... 0.460)	0.14 (-0.017 ... 0.31)	54.355

slightly higher in May, so this may have had an influence as well. In the ENEB, the precipitation is strongly modulated by Easterly Waves Disturbances (EWD) (Amorim et al., 2014; Gomes et al., 2015; Gomes et al., 2019; Neves et al., 2016; Kouadio et al., 2012; Ramos, 1975; Torres and Ferreira, 2011; da Silva et al., 2020) with maximum rainfall between May and July, and annual average precipitation above 1500 mm. SST anomalies over Tropical South Atlantic (TSA) and El Niño Southern Oscillation (ENSO) that interact with global circulation modulate the rainfall variability in the ENEB (Andreoli and Kayano, 2007; Silva et al., 2018; Silva & Guedes, 2012; Torres and Ferreira, 2011; Rodrigues et al., 2020). The very intense daily rainfall events of May 2022 were largely caused by the propagation of EWD (Vale Silva et al., 2023), which in combination with an anomalously warm tropical Atlantic and a humid and unstable atmosphere near the east coast of Northeast Brazil favoured the development and propagating of very convective precipitation clouds, with expressive values of vertical velocity and relative humidity at 700 hPa near the NEB's coast in a sequence of days, as illustrated in Fig. 2(c).

4. Model evaluation

In the subsections below we show the results of the model validation for the 7-day and the 15-day events. To validate the quality of the models, we firstly qualitatively compare the seasonal cycles in models and observations. The seasonal cycle is labeled 'reasonable' if it has one peak extending in time to at least May. We note that convective warm rains are not represented well in most of the models, with the precipitation seasonal cycles declining around May, thus missing the warm rain season from May–Aug. The only exception is CNRM-CM6-1-HR from the HighResMIP experiment, where the seasonal cycle is consistent with the observed cycle (Fig. S1 for observations; Fig. S3 (a-c) for climate models). Secondly, we compare the spatial pattern of annual rainfall. For the spatial patterns we compare, again visually, the average precipitation over March to August in the observations with those in the models. Thirdly, we compare the parameters of the fitted GEV in observations and models. If the parameter best estimate of the model is inside the range of the parameter range of observations, it is labeled 'good', it is labeled 'reasonable' if there is only some overlap, and it is labeled 'bad' if there is no overlap between the parameter ranges.

5. Multi-method multi-model attribution

This section shows Probability Ratios and change in intensity ΔI for models that passed the validation tests and also includes the values calculated from the fits with observations. All models labeled 'reasonable' or 'good' have been included, although we note that these models all miss some essential physics.

6. Hazard synthesis

For both the 7-day annual maximum and the 15-day annual maximum precipitation we calculate the probability ratio as well as the change in magnitude of the event in the observations and the models. If the models do not pass the validation tests, we do not use the results. We synthesise the ones that pass with the observations to give an overarching attribution statement. Figs. 9 and 10 show the changes in probability and intensity for the observations (blue) and models (red). The width of the colored bars show a measure of the natural variability in the observations and models as obtained with the bootstrap procedure in the GEV fitting. Before combining them into a synthesised assessment, a term to account for intermodel spread is added (in quadrature) to the natural variability of the models. This is shown as white boxes around the light red bars in Figs. 9 and 10. The dark red bar is the model average that takes both model natural variability and intermodel spread into account. Next, observations and models are combined into a single result in two ways. Firstly, we neglect common model uncertainties beyond the model spread that is depicted by the model average, and compute the weighted average of the model average and observations: this is indicated by the magenta bar. As, due to common model uncertainties, model uncertainty can be larger than the model spread, secondly, we also show the more conservative estimate of an unweighted average of observations and the model average, indicated by the white box around the magenta bar in the synthesis figures.

The tendency towards heavier precipitation in the 7-day and 15-day time scales in the observed data, albeit large uncertainties due to natural variability (blue bars in Figs. 9 and 10), aligns with the effects of global warming. This behaviour is consistent with the scientific understanding described by the Clausius-Clapeyron relationship, that a warmer atmosphere can hold more moisture. This tendency is not replicated in the models, possibly due to the models not capturing the convective processes that are important for this region (discussed in Section 2.2 and Section 4). Therefore, even those model runs that passed our validation tests and included in the attribution analysis are considered to be of limited value only (shown by red bars in Figs. 9 and 10). Moreover, the model estimates of changes in intensity and probability do not show a consistent change. It is important to note that this is an artefact of the models and not an indication of the real-world changes. We first need to improve the representation of this type of warm rainfall in models before we can present model results with more confidence. Because of the model deficiencies we cannot use the synthesised values that combine observations and models.

According to the IPCC AR6 (Seneviratne et al., 2021), the change in average precipitation over Northeast Brazil is more likely to decrease, in addition to an increase in the occurrence of consecutive dry days, however the projection of extreme rainfall events goes in the opposite direction, with uniform increasing of the largest daily precipitation in a year. By combining observations with these alternate lines of evidence and the physical understanding of the climate system, we conclude that human-induced climate change is, at least in part, responsible for the increase in likelihood and intensity of heavy rainfall events as observed in May 2022, although we cannot quantify the role of climate change.

7. Vulnerability and exposure

In addition to assessing the changing risk of the rainfall that contributed to the flood hazard, in this section we look at the vulnerability and exposure factors that increased the likelihood of impacts in the affected region.

Despite Brazil's significant socio-economic progress (e.g., 29 million people lifted out of poverty between 2003 and 14), inequality, disparities, marginalisation and displacement remain major drivers of vulnerability to disasters (Kakinuma et al., 2020; Lemos et al., 2016; Dolman et al., 2018), further amplified by climate change impacts (Debortoli et al., 2017; Rasch, 2016). Vulnerabilities and their implications are unequally distributed across rural/urban divides and ethnicities (Gubert et al., 2017; Oliveira et al., 2020).

Northeast Brazil is the country's poorest and least developed region (Hummell et al., 2016). It has the lowest average municipality equivalized median monthly household income at R$ 429 (Rasch, 2017). Cities and urban planning can highlight underlying inequities especially for marginalised or disadvantaged ethnic groups and residents of slave-descendant communities (Gubert et al., 2017).

7.1. History of floods

The Pernambuco and Alagoas states, and in particular their coastal areas, have a long history of flooding. The risk of recurring floods is well-known among affected communities (Ardaya et al., 2017). For example, floods in 2010 mainly impacted these two states and resulted in entire villages being destroyed, 120,000 people displaced and destruction of roads, bridges, ICT infrastructure and more (Relief Web, 2010). In Pernambuco, the losses and damages were estimated at R$ 3,4 billion

Table 4
Evaluation results for the climate models considered for the attribution analysis of annual maximum 15-day rainfall in the year 2022, over the study region. The table contains qualitative assessments of seasonal cycle and spatial pattern of precipitation from the models (good, reasonable, bad) along with estimates for dispersion parameter, shape parameter and event magnitude. The corresponding estimates for observations are shown in blue. Based on overall suitability, the models are classified as reasonable and bad, shown by yellow and red highlights, respectively.

Observations	Seasonal cycle	Spatial pattern	Dispersion	Shape parameter	Event magnitude
Station			0.243 (0.188 ... 0.290)	-0.23 (-0.48 ... -0.084)	23.95
Model					**Threshold for 1000-yr return period**
FLOR historical-rcp45 (5)	reasonable, drops early in the season	Good	0.235 (0.213 ... 0.249)	-0.078 (-0.20 ... -0.029)	31.702
CNRM-CM6-1-HR HighResMIP (1)	good	Good	0.142 (0.111 ... 0.168)	0.089 (-0.10 ... 0.24)	25.141
EC-Earth3P-HR HighResMIP (1)	reasonable	Good	0.271 (0.210 ... 0.315)	-0.011 (-0.23 ... 0.17)	14.484
HadGEM3-GC31-HM HighResMIP (1)	reasonable	reasonable	0.257 (0.182 ... 0.305)	-0.14 (-0.32 ... 0.048)	28.53
HadGEM3-GC31-MM HighResMIP (1)	reasonable	reasonable	0.275 (0.227 ... 0.313)	0.073 (-0.11 ... 0.21)	32.734
AM2.5C360 AMIP (10)	reasonable, drops early in the season	Good	0.277 (0.254 ... 0.299)	-0.043 (-0.11 ... 0.017)	37.222
MPI-ESM-MR/ REMO2015 CORDEX SAM-22 (1)	bad	Bad	0.159 (0.113 ... 0.194)	-0.18 (-0.48 ... 0.047)	27.019
NorESM1-M / REMO2015 CORDEX SAM-22 (1)	reasonable	reasonable	0.246 (0.188 ... 0.288)	-0.15 (-0.38 ... 0.018)	18.967
MPI-ESM-MR / RegCM4-7 CORDEX SAM-22 (1)	bad	Bad	0.341 (0.259 ... 0.401)	0.32 (0.077 ... 0.58)	147.17
NorESM1-M / RegCM4-7 CORDEX SAM-22 (1)	reasonable	reasonable	0.578 (0.459 ... 0.674)	-0.21 (-0.79 ... 0.21)	60.047
MPI-ESM-LR / REMO2009 CORDEX SAM-44 (1)	bad	Bad	0.196 (0.153 ... 0.231)	-0.19 (-0.39 ... 0.015)	28.936
CSIRO-Mk3-6-0 / SMHI-RCA4 CORDEX SAM-44 (1)	bad	Bad	0.117 (0.0920 ... 0.139)	0.030 (-0.22 ... 0.27)	10.389
EC-EARTH / SMHI-RCA4 CORDEX SAM-44 (1)	bad	Bad	0.163 (0.127 ... 0.190)	0.10 (-0.18 ... 0.33)	42.4
IPSL-CM5A-MR / SMHI-RCA5 CORDEX SAM-44 (1)	reasonable	Bad	0.251 (0.180 ... 0.301)	-0.12 (-0.30 ... 0.062)	41.431
MIROC5 / SMHI-RCA4 CORDEX SAM-44 (1)	reasonable	reasonable	0.257 (0.211 ... 0.306)	-0.095 (-0.46 ... 0.14)	32.603
HadGEM2-ES / SMHI-RCA4 CORDEX SAM-44 (1)	reasonable	reasonable	0.311 (0.238 ... 0.379)	-0.39 (-0.75 ... -0.26)	27.893
MPI-ESM-LR / SMHI-RCA4 CORDEX SAM-44 (1)	bad	Bad	0.221 (0.175 ... 0.263)	-0.18 (-0.51 ... -0.012)	30.67
NorESM1-M / SMHI-RCA4 CORDEX SAM-44 (1)	reasonable	reasonable	0.355 (0.273 ... 0.416)	-0.068 (-0.28 ... 0.12)	34.438
GFDL-ESM2M / SMHI-RCA4 CORDEX SAM-44 (1)	bad	Bad	0.211 (0.160 ... 0.248)	0.090 (-0.10 ... 0.30)	55.91
CanESM2 / UCAN_WRF341I CORDEX SAM-44 (1)	reasonable	reasonable	0.366 (0.285 ... 0.427)	0.13 (-0.096 ... 0.31)	43.094

(World Bank, 2012a), while in Alagoas resulted in R$ 1,89 billion (World Bank 2012b).

In 2017 another flood in the same states resulted in local states of emergency being declared and over 55,000 people displaced. Between 1995 and 2019, Pernambuco had accumulated losses in disasters that reached R$ 29,1 billion - the fourth position between the 27 federative units in Brazil - while Alagoas had R$ 8,9 billion - the 15th position (World Bank 2020). The number of housing units destroyed in disasters were 20,300 in Pernambuco (3rd position in the country) and 16,400 in Alagoas (6th position) (World Bank 2020). Over the past years, several participatory actions including crowd-sourcing geo-information have been piloted to improve flood risk management (Mansur et al., 2018; Horita et al., 2015; Degrossi et al., 2014).

7.2. Land-use planning and urbanisation

Situated on the coast of the Atlantic Ocean at the confluence of the Capibaribe and Beberibe rivers and over 70 channels, the Metropolitan Region of Recife (MRR) was amongst the hardest hit by the 2022 flood. Recife, the state capital of Pernambuco, is one of the cities with the highest flood risk in Brazil with high population density (7,602 people/km2) and poverty rates (40 percent) paired with significant Black, Brown and Indigenous communities (approximately 59 percent combined) (Hummell et al., 2016; City Population 2021; Global Future Cities, n.d.; IBGE, 2010).

The region has seen rapid urbanisation and increased population density caused by population increases and migration. The broader northeast Brazil region is subject to recurring droughts that have resulted in mass migrations to already overcrowded urban centers (Marengo et al., 2021). For instance, between 1950 and 2000, the urban population of Recife tripled (IBGE, 2020) - based on the 2010 National Census, there were 1,5 million people living in the city which has landscape characteristics (low average altitude, flat areas, a water table close to the surface) which make it particularly exposed to hydrometeorological hazards (Souza Leao et al., 2021). According to the census, 13.4% of the city's populations lives in high and very high risk-prone areas: Of 644, 620 people living in Jaboatão dos Guararapes, 29.2% are settled in landslide or flood-prone areas mapped by the Brazilian Geological Survey (IBGE 2018).

In line with other regions in Brazil, the urban front expands with little oversight and planning, and often results in concentration of informal settlements on flood-prone areas or on/near steep slopes at risk of landslides (Gomes et al., 2012). Many of the rural migrants live in informal settlements which presently make up nearly one-fourth of the Metropolitan Region of Recife's 3,7 million residents (Koster, 2020). Falling beyond official municipal boundaries, homes in these informal settlements are often situated on steep hillslopes and along floodplains (Marengo et al., 2021). The houses built are often shacks made of wood, metal sheets, mud bricks, without a foundation established on firm ground (bedrock). This, coupled with the removal of vegetation, destabilises the soil making it prone to landslides when soaked, a phenomenon documented in several hills in the Recife municipality (Lins et al., 2020).

The creation of impervious surface and changes to local hydrology and geology has also had an impact on increasing flood and landslide risk, hampering the effectiveness of drainage and sanitation systems, and increasing flood risk (Souza Leao et al., 2021; Cerqueira et al., 2020). Urban sanitation and drainage infrastructure is inadequate, usually due to a lack of planning and assessments deemed incompatible to current needs of most cities around the country (Rodrigues et al., 2022).

7.3. Risk management - preparedness, early warning early action, and response

Planning and preparedness play a key role in reducing the vulnerability and exposure of people and assets during disasters.

In Brazil, different flood risk management laws and policies exist at national, state, and municipal scale. For instance, 1,538 (27.6%) of 5,570 municipalities have urban plans which take into account flood risks (IBGE 2020) - in the Northeast region, 18.7% of municipalities have these plans. Brazil's National Center for Monitoring and Early Warning of Natural Disasters (CEMADEN) was created in July 2011, after the devastating Petropolis floods and landslides (Marchezini et al., 2017). Sitting at the Ministry of Science, Technology and Innovation, CEMADEN currently monitors 1038 cities in Brazil - with landslide and flood maps which were developed by the Brazilian Geological Survey (CPRM, 2022) - and is responsible for issuing alerts to the National Secretariat of Civil Defense (SEDEC).

The State of Pernambuco's Water and Climate Agency (APAC) also has a flood early warning system by which alerts are issued to the public. The warnings range from yellow to orange to red, a combination of probability of occurrence and intensity of rain events (APAC, 2022). APAC also participates in the training of Municipal Civil Defences, explaining how the weather forecasts work and the three types of alerts (yellow, orange and red), based on the daily weather forecasting and tendencies updates. All representatives of the municipal Civil Defences have direct communication with the APAC Situation Room, and from these updates and trainings, each municipality is responsible for updating its disaster risk reduction (DRR) and contingency plan annually - 24.3% of cities have DRR plans in Pernambuco (IBGE, 2020). In addition to media outlets, policies enacted in response to previous flood events enabled the alerts to be issued through SMS, although the text of a current bill under consideration by the Recife Assembly suggests these SMS warnings are "unavailable", justifying the introduction of this additional bill to strengthen Recife's response programs. Finally, each municipality is responsible for developing procedures for preventive measures in case of disasters. Every year, the members of the Municipal Civil Defences are trained to update such measures for the rainy season in the State of Pernambuco.

For this event, the severe rainfall that contributed to the floods and landslides was relatively well-forecasted albeit with a wide range, with sources such as GLOFAS forecasting flooding between a 2–5-year average to over a 20 year average (Start Network, May 27, 2022; ECHO, May 31, 2022). Conditions were monitored by agencies such as APAC (internal communication) and warning alerts were issued - notably, the municipal government of Recife issued a red alert for heavy rainfall on May 27. Technical meetings were held between APAC and Pernambuco Civil Defense to support prevention actions based on weather and climate conditions. Federal, State and Municipal disaster response included search and rescue, first aid provision, and the restoration of essential services, all of which would have reduced the impacts of the events once they had occurred (MDR. Ministério do Desenvolvimento Regional, 2022). Pernambuco State Government has announced plans to also provide financial support for disaster recovery to the affected population.

Recent research also points to potential policy implementation gaps that may need improvement to increase the effectiveness of climate and disaster risk reduction policies and structures. Political action has historically followed on the heels of large disasters and this reactive approach to the challenges has not (yet) led to a complete integration of all levels and links in the warning systems chain. This is a politically charged issue made more complex in times of political instability and economic recession. If left unresolved, this situation may contribute to increasing vulnerability and risks of disasters.

8. Conclusions

A rapid attribution study was performed to assess the role of climate change in altering the likelihood and intensity of the extreme rainfall over a land area of coastal Eastern Northeast Brazil (10°S-5°S; 36°W-45.5°W) that encompasses the region impacted by the observed extreme

Table 5
Precipitation threshold for the 500-yr return period 7-day annual maximum precipitation, Probability Ratio and change in intensity for the models that passed the validation tests, for the study region.

Model/Observations	Threshold for return period 500 yr	Probability ratio PR [−]	Change in intensity ΔI [%]
75 stations	33.95 mm/day	4.3e+4 (1.7 … ∞)	27 (0.95 … 59)
FLOR historical-rcp45 (5)	45 mm/day	1.5 (1.1 … 2.0)	3.5 (0.71 … 6.4)
CNRM-CM6-1-HR HighResMIP (1)	28 mm/day	0.27 (0.0020 … 43)	−11 (−23 … 5.0)
EC-Earth3P-HR HighResMIP (1)	20 mm/day	0.49 (0.0092 … 9.8)	−8.5 (−33 … 25)
HadGEM3-GC31-HM HighResMIP (1)	38 mm/day	54 (0.089 … ∞)	18 (−15 … 55)
HadGEM3-GC31-MM HighResMIP (1)	45 mm/day	0.91 (0.057 … 25)	−1.4 (−28 … 30)
AM2.5C360 AMIP (10)	48 mm/day	0.74 (0.18 … 2.2)	−2.6 (−12 … 6.4)
NorESM1-M/REMO2015 CORDEX SAM-22 (1)	29 mm/day	0.15 (0.000077 … ∞)	−19 (−37 … 14)
MIROC5/SMHI-RCA4 CORDEX SAM-44 (1)	59 mm/day	4.1 (0.19 … 5.1e+5)	19 (−10 … 63)
HadGEM2-ES/SMHI-RCA4 CORDEX SAM-44 (1)	38 mm/day	∞ (2.5e+2 … ∞)	16 (−0.23 … 35)

Table 6
Precipitation threshold for the 1000-yr return period 15-day annual maximum precipitation, Probability Ratio and change in intensity for the models that passed the validation tests, for the study region.

Model/Observations	Threshold for return period 1000 yr	Probability ratio PR	Change in intensity ΔI [%]
75 stations	23.94 mm/day	∞ (0.12 … ∞)	15 (−7.5 … 47)
FLOR historical-rcp45 (5)	32 mm/day	1.7 (1.2 … 3.0)	3.6 (1.5 … 6.1)
EC-Earth3P-HR HighResMIP (1)	14 mm/day	0.57 (0.015 … 1.7e+3)	−5.0 (−28 … 26)
HadGEM3-GC31-HM HighResMIP (1)	29 mm/day	5.4 (0.019 … ∞)	7.0 (−15 … 37)
HadGEM3-GC31-MM HighResMIP (1)	33 mm/day	0.49 (0.0045 … 5.6)	−9.3 (−33 … 17)
AM2.5C360 AMIP (10)	37 mm/day	0.58 (0.095 … 2.3)	−4.2 (−15 … 7.3)
NorESM1-M/REMO2015 CORDEX SAM-22 (1)	19 mm/day	0.020 (0.0000080 … ∞)	−23 (−41 … −0.83)
MIROC5/SMHI-RCA4 CORDEX SAM-44 (1)	33 mm/day	42 (0.67 … ∞)	18 (−8.6 … 50)
HadGEM2-ES/SMHI-RCA4 CORDEX SAM-44 (1)	28 mm/day	∞ (14 … ∞)	10 (−4.4 … 25)
NorESM1-M/SMHI-RCA4 CORDEX SAM-44 (1)	34 mm/day	0.32 (0.00024 … ∞)	−9.0 (−35 … 32)

events of May 2022. Trend and extreme value analysis were performed using 7 and 15-day mean maximum values using consistent and regularly distributed observed data of 75 stations since the 1970s. The same assessment was performed using state-of-the-art climate models in a 1.2 °C colder climate than the current conditions.

The rainfall that resulted in flash floods in coastal northeastern Brazil was very rare (a 1–500 to 1–1000 year event for the 7 and 15-day mean, respectively), and one can reasonably assume that such a rare event will be an impactful one. Even though both events were located far outside range of the previously observed records, because of the short observational record and associated uncertainties it was not possible to quantify how much climate change made these events more likely to happen. The performed analysis also revealed that global warming increased the intensity of such extreme rainfall: rainfall events as rare as those investigated here occurring in a 1.2 °C cooler climate would have been approximately a fifth less intense.

While many climate models simulate the main precipitation features over the region, we find that for such spatially local events, all models exhibit systematic errors in precipitation magnitudes. This is partly due to their coarse spatial resolution and misrepresentation of key physical processes (e.g., convection and associated warm rains), which hinders our ability to quantify the role of climate change in the observed increase in likelihood and intensity of such extreme events. However, evidence from previous studies (e.g., Seneviratne et al., 2021) and the physical understanding of the climate system indicates that extreme rainfall in the region will increase under warming; therefore we conclude that human-induced climate change is, at least in part, responsible for the increase in likelihood and intensity of heavy rainfall events as observed in May 2022.

The extreme nature of the floods made it so that exposure was the main determinant of impact, although long-term impacts and recovery will likely be mediated by socio-economic, demographic and governance factors. An increase in urbanisation, especially unplanned and informal in low-lying flood-prone areas and steep hillsides have increased the community exposure to these hazards. The need for improving the linkage between early warning and prevention actions is highlighted. It is unclear to what extent the warning helped reduce the impacts, even though some actions were taken by Civil Defense. However, it was not possible to prevent fatalities because of the magnitude of the extreme rainfall events. This indicates the need to review and strengthen the protocols between weather warnings and the process that would lead to improved anticipatory action based on those warnings. This region also generally has an infrastructure deficit (e.g., housing, roads, water and sanitation etc.). As new infrastructure is built, there is an opportunity to increase resilience by accounting for increasing risks in the design and location, instead of reverting to outdated design standards.

CRediT authorship contribution statement

Francisco das Chagas Vasconcelos Junior: Data curation, Formal analysis, Supervision, Writing – original draft, Writing – review & editing. **Mariam Zachariah:** Data curation, Formal analysis, Investigation, Methodology, Writing – original draft, Writing – review & editing. **Thiago Luiz do Vale Silva:** Data curation, Formal analysis, Validation. **Edvânia Pereira dos Santos:** Data curation, Formal analysis. **Caio.A.S. Coelho:** Conceptualization, Data curation, Formal analysis, Investigation, Supervision, Validation, Visualization, Writing – original draft, Writing – review & editing. **Lincoln M. Alves:** Formal analysis, Writing – original draft, Writing – review & editing. **Eduardo Sávio Passos Rodrigues Martins:** Data curation, Formal analysis, Supervision, Writing – original draft. **Alexandre C. Köberle:** Investigation, Writing – original draft, Writing – review & editing. **Roop Singh:** Data curation, Formal analysis, Investigation, Methodology. **Maja Vahlberg:** Data curation, Formal analysis, Investigation, Methodology. **Victor Marchezini:** Writing – original draft, Writing – review & editing. **Dorothy Heinrich:** Conceptualization, Data curation, Formal analysis, Investigation, Writing – original draft, Writing – review & editing. **Lisa Thalheimer:** Conceptualization, Data curation, Methodology, Supervision, Visualization, Writing – original draft, Writing – review & editing. **Emmanuel Raju:** Validation, Visualization, Writing – original draft, Writing – review & editing. **Gerbrand Koren:** Data curation, Formal analysis, Investigation, Visualization, Writing – original draft, Writing – review & editing. **Sjoukje Y. Philip:** Conceptualization, Data curation,

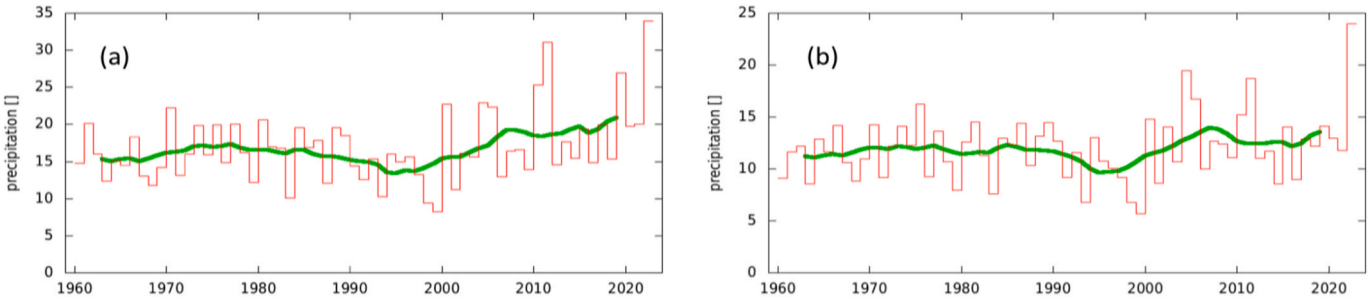

Fig. 6. Time series of annual (a) 7-day maximum precipitation in [mm/day] and (b) 15-day maximum precipitation in [mm/day] averaged over the selected 75 precipitation stations. The green line shows the 10-year running mean. (For interpretation of the references to color in this figure legend, the reader is referred to the Web version of this article.)

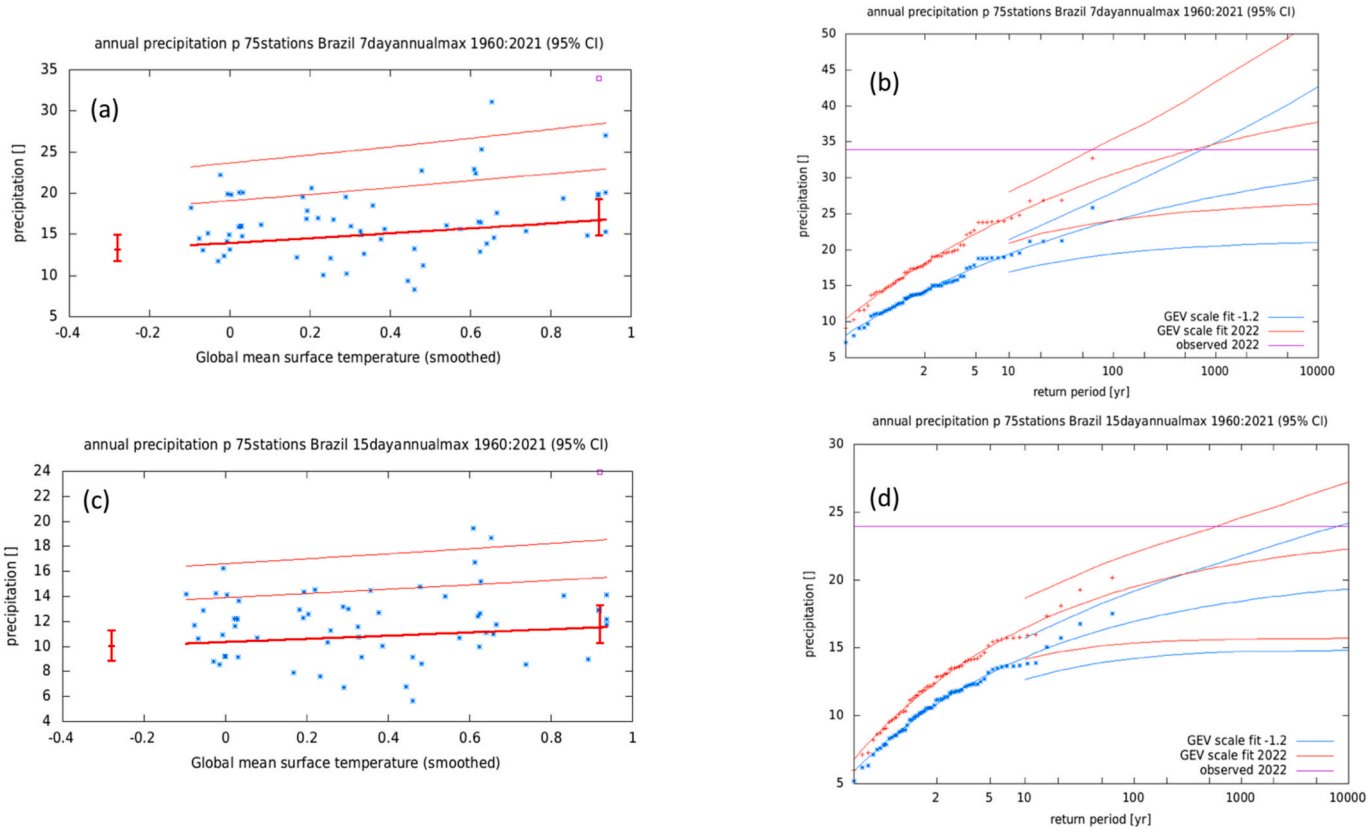

Fig. 7. (a) GEV fit with constant dispersion parameter, and location parameter scaling proportional to GMST, for the average over 75 stations. No information from 2022 is included in the fit. Left: Annual maximum 7-day (a) and 15-day (c) average rainfall (in mm/day) as a function of the smoothed GMST. The thick red line denotes the time-varying location parameter and the thin lines are 1 and 2 standard deviations above. The vertical red lines show the 95% confidence interval for the location parameter, for the current, 2022 climate and the fictional, 1.2 °C cooler climate. The 2022 observation is highlighted with the magenta box. Right: Return time plots for the climate of 2022 (red) and a climate with GMST 1.2 °C cooler (blue), for the annual maximum 7-day average (b) and the 15-day average (d) rainfall (in mm/day). The past observations are shown twice: once shifted up to the current climate and once shifted down to the climate of the late nineteenth century. The markers show the data and the lines show the fits and uncertainty from the bootstrap. The horizontal magenta line shows the magnitude of the 2022 event analysed here. The thin red lines in panels a and c show 1 standard deviation (s.d.) and 2 s.d. above the thick red lines. (For interpretation of the references to color in this figure legend, the reader is referred to the Web version of this article.)

Formal analysis, Investigation, Methodology, Resources, Software, Validation, Visualization, Writing – original draft, Writing – review & editing. **Sarah F. Kew:** Data curation, Formal analysis, Investigation, Methodology, Software, Validation, Visualization, Writing – original draft, Writing – review & editing. **Rémy Bonnet:** Data curation, Formal analysis, Investigation, Methodology, Validation, Visualization, Writing – original draft, Writing – review & editing. **Sihan Li:** Data curation, Formal analysis, Investigation, Methodology, Software, Validation. **Wenchang Yang:** Data curation, Formal analysis, Methodology, Software, Visualization, Writing – original draft. **Jingru Sun:** Investigation, Methodology, Writing – original draft, Writing – review & editing. **Gabriel Vecchi:** Data curation, Formal analysis, Validation, Visualization. **Friederike.E.L. Otto:** Conceptualization, Data curation, Formal analysis, Funding acquisition, Resources, Software, Supervision, Validation.

Declaration of competing interest

The authors declare that they have no known competing financial interests or personal relationships that could have appeared to influence

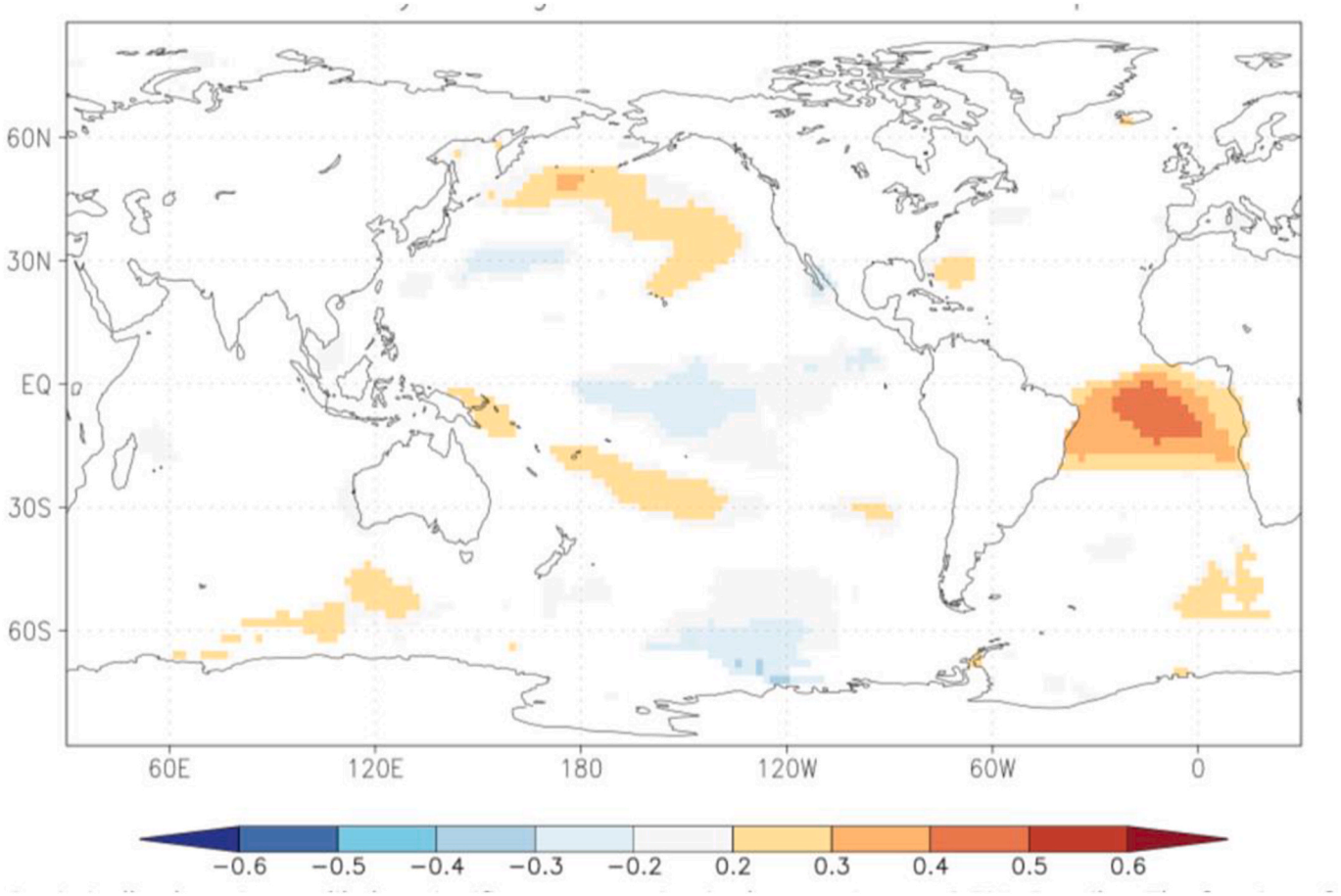

Fig. 8. Correlation between rainfall (from GPCC dataset) over the eastern Northeast region in Brazil and global ERSST Sea Surface Temperatures for months Mar–May, calculated over years 1891–2022.

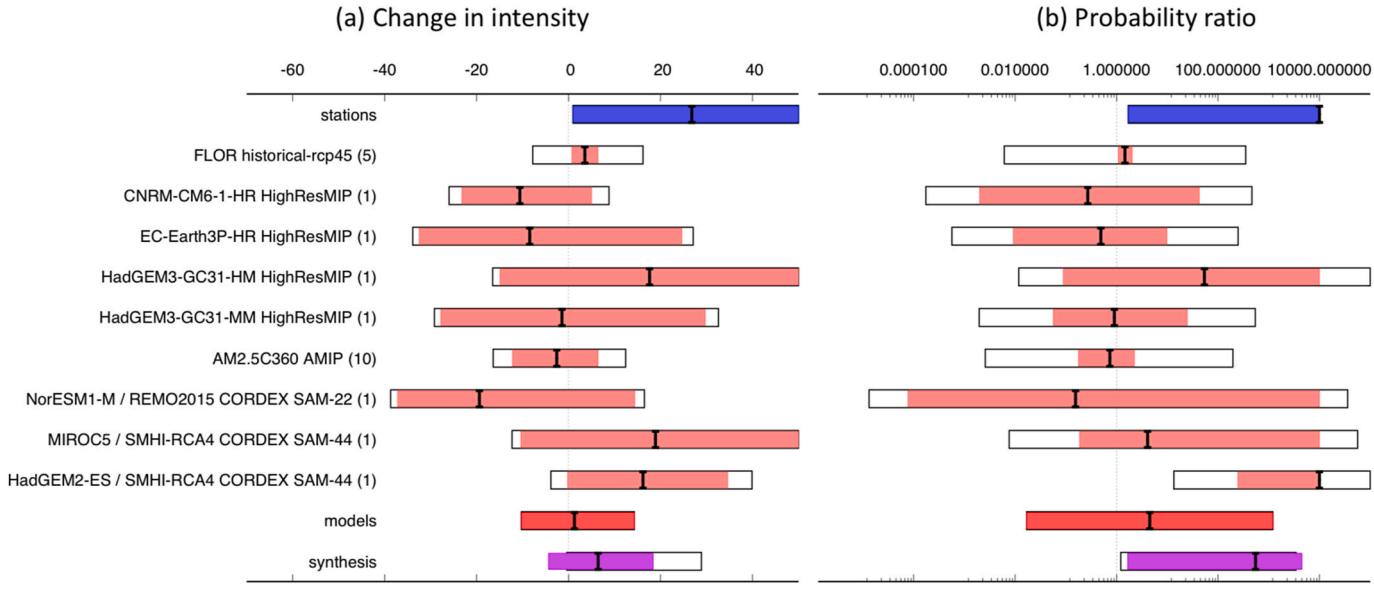

Fig. 9. Synthesis of intensity change (left) and probability ratios (right), when comparing the 7-day annual maximum event with a 1.2degC cooler climate.

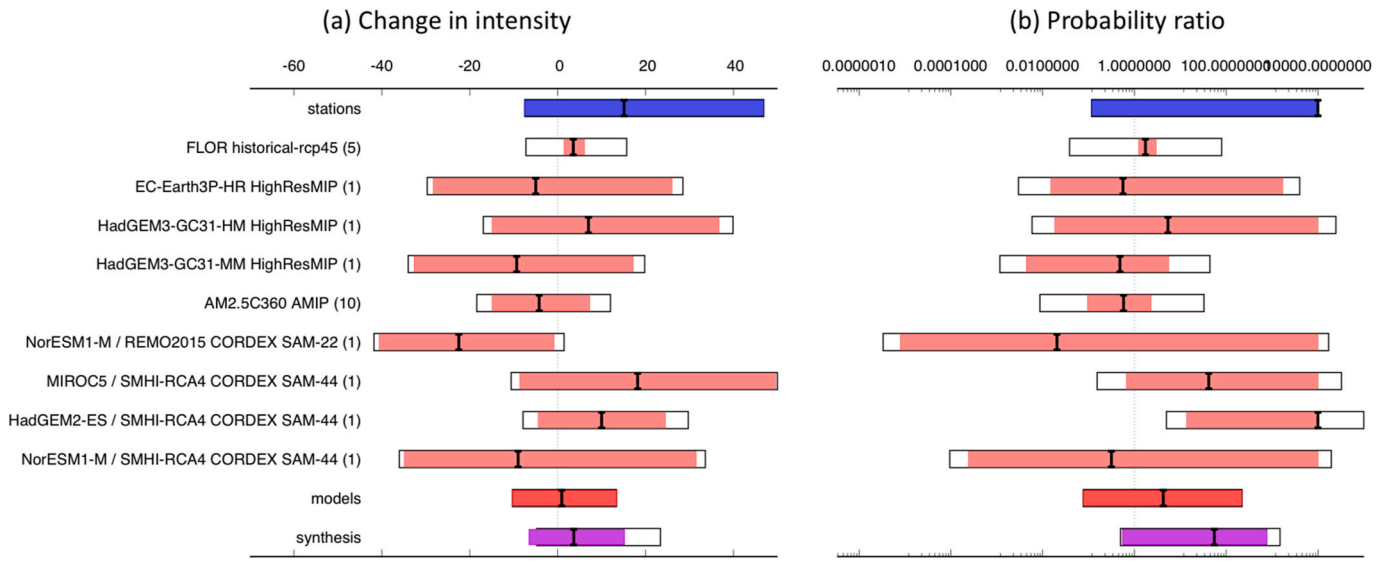

Fig. 10. Synthesis of intensity change (left) and probability ratios (right), when comparing the 15-day annual maximum event with a 1.2degC cooler climate.

the work reported in this paper.

Data availability

Data will be made available on request.

Acknowledgments

The authors would like to thank the National Institute of Meteorology (INMET), the National Water and Sanitation Agency (ANA), and all Regional Met Centers of Northeast Brazil for making available the rainfall data used in this study. First author thanks the National Council for Scientific and Technological Development - CNPq (grants 409666/2021-1 and 316867/2023-3).

Appendix A. Supplementary data

Supplementary data to this article can be found online at https://doi.org/10.1016/j.wace.2024.100699.

References

Alvares, C.A., Stape, J.L., Sentelhas, P.C., de Moraes, G., Leonardo, J., Sparovek, G., 2013. Koppen's Climate classification maps for Brazil. Meteorol. Z. 22 (6), 711–728. https://doi.org/10.1127/0941-2948/2013/0507.

Amorim, Ana Cleide Bezerra, Chaves, Rosane Rodrigues, Silva, Cláudio Moisés Santos e, 2014. Influence of the tropical Atlantic Ocean's Sea Surface temperature in the Eastern Northeast Brazil precipitation. Atmospheric And Climate Sciences, [s. l.] 4 (5), 874–883. https://doi.org/10.4236/acs.2014.45077. ISSN 2160-0422 versão online. https://www.scirp.org/pdf/ACS_2014112611293471.pdf.

Andreoli, R.V., Kayano, M.T., 2007. A importância relativa do Atlântico Tropical sul e pacífico leste na variabilidade de precipitação do Nordeste do Brasil. Rev. Bras. Meteorol. 22 (1), 63–74. https://doi.org/10.1590/S0102-77862007000100007.

Ardaya, A.B., Evers, M., Ribbe, L., 2017. What influences disaster risk perception? Intervention measures, flood and landslide risk perception of the population living in flood risk areas in Rio de Janeiro state, Brazil. Int. J. Disaster Risk Reduc. 25, 227–237. https://doi.org/10.1016/j.ijdrr.2017.09.006.

Cerqueira, T.C., Mendonça, R.L., Gomes, R.L., de Jesus, R.M., da Silva, D.M.L., 2020. Effects of urbanization on water quality in a watershed in northeastern Brazil. Environ. Monit. Assess. 192 (1), 1–17. https://doi.org/10.1007/s10661-019-8020-0.

Chan, D., Vecchi, G.A., Yang, W., Huybers, P., 2021. Improved simulation of 19th-and 20th-century North Atlantic hurricane frequency after correcting historical sea surface temperatures. Sci. Adv. 7, eabg6931 https://doi.org/10.1126/sciadv.abg6931.

Ciavarella, A., Cotterill, D., Stott, P., Kew, S., Philip, S., van Oldenborgh, G.J., et al., 2021. Prolonged Siberian heat of 2020 almost impossible without human influence. Climatic Change 166 (1), 9. https://doi.org/10.1007/s10584-021-03052-w.

City Population. Population of recife city. https://www.citypopulation.de/en/brazil/regiaonordeste/admin/pernambuco/2611606_recife/. (Accessed 1 July 2021).

Civil Defense- Alagoas, 2022. Personal Communication on 27 June 2022. Maceió.

Civil Defense- Pernambuco, 2022. By Secretary of Pernambuco. Recife. Daily report on 27.

Costa, M.B.S.F., Mallmann, D.L., Pontes, P.M., Araujo, M., 2010. Vulnerability and impacts related to the rising sea level in the Metropolitan Center of Recife, Northeast Brazil. Pan Am. J. Aquat. Sci. 5 (2), 341–349. Retrieved from. https://panamjas.org/pdf_artigos/PANAMJAS_5(2)_341-349.pdf.

Debortoli, N.S., Camarinha, P.I.M., Marengo, J.A., Rodrigues, R.R., 2017. An index of Brazil's vulnerability to expected increases in natural flash flooding and landslide disasters in the context of climate change. Nat. Hazards 86 (2), 557–582. https://doi.org/10.1007/s11069-016-2705-2.

Degrossi, L.C., de Albuquerque, J.P., Fava, M.C., Mendiondo, E.M., 2014. Flood Citizen Observatory: a crowdsourcing-based approach for flood risk management in Brazil. SEKE 570–575.

Delworth, T.L., Rosati, A., Anderson, W., Adcroft, A.J., Balaji, V., Benson, R., Dixon, K., Griffies, S.M., Lee, H.-C., Pacanowski, R.C., Vecchi, G.A., Wittenberg, A.T., Zeng, F., Zhang, R., 2012. Simulated climate and climate change in the GFDL CM2.5 high-resolution coupled climate model. J. Clim. 25, 2755–2781. https://doi.org/10.1175/JCLI-D-11-00316.1.

Dolman, D.I., Brown, I.F., Anderson, L.O., Warner, J.F., Marchezini, V., Santos, G.L.P., 2018. Re-thinking socio-economic impact assessments of disasters: the 2015 flood in Rio Branco, Brazilian Amazon. Int. J. Disaster Risk Reduc. 31, 212–219. https://doi.org/10.1016/j.ijdrr.2018.04.024.

Giorgi, F., Coppola, E., Teichmann, C., Jacob, D., 2021. Editorial for the CORDEX-CORE experiment I special issue. Clim. Dynam. 57, 1265–1268. https://doi.org/10.1007/s00382-021-05902-w.

Global Future Cities. Global Future Cities. Recife, Republic Federative of Brazil. https://www.globalfuturecities.org/federative-republic-brazil/cities/recife, (n.d.).

Gomes, J.H., do Vale Silva, T.L., Guerra, E.R., Dias, D.T., 2012. Ocupação em Área de Risco de Deslizamentos no Córrego do Jenipapo, Recife, Pernambuco. Revista Brasileira de Geografia Física 3, 524–539. https://doi.org/10.26848/rbgf.v5i3.232849.

Gomes, H.B., Ambrizzi, T., Herdies, D.L., Hodges, K., Pontes da Silva, B.F., 2015. Easterly wave disturbances over Northeast Brazil: an observational analysis. Adv. Meteorol. 2015, 1–20. https://doi.org/10.1155/2015/176238.

Gomes, Helber B., Ambrizzi, Tércio, Pontes da Silva, Bruce F., Hodges, Kevin, Silva Dias, Pedro L., Herdies, Dirceu L., Silva, Maria Cristina L., Gomes, Heliofábio B., 2019. Climatology of easterly wave disturbances over the tropical South Atlantic. Clim. Dynam. 53, 1393–1411.

Grimm, A.M., 2011. Interannual climate variability in South America: impacts on seasonal precipitation, extreme events, and possible effects of climate change. Stoch. Environ. Res. Risk Assess. 25, 537–554.

Gubert, M.B., Segall-Corrêa, A.M., Spaniol, A.M., Pedroso, J., Coelho, S.E.D.A.C., Pérez-Escamilla, R., 2017. Household food insecurity in black-slaves descendant communities in Brazil: has the legacy of slavery truly ended? Publ. Health Nutr. 20 (8), 1513–1522. https://doi.org/10.1017/S1368980016003414.

Gutowski, W.J., Giorgi, F., Timbal, B., Frigon, A., Jacob, D., Kang, H.-S., Raghavan, K., Lee, B., Lennard, C., Nikulin, G., O'Rourke, E., Rixen, M., Solman, S., Stephenson, T., Tangang, F., 2016. WCRP COordinated regional downscaling EXperiment (CORDEX): a diagnostic MIP for CMIP6. Geosci. Model Dev. (GMD) 9, 4087–4095. https://doi.org/10.5194/gmd-9-4087-2016.

Haarsma, R.J., Roberts, M.J., Vidale, P.L., Senior, C.A., Bellucci, A., Bao, Q., Chang, P., Corti, S., Fučkar, N.S., Guemas, V., von Hardenberg, J., Hazeleger, W., Kodama, C., Koenigk, T., Leung, L.R., Lu, J., Luo, J.-J., Mao, J., Mizielinski, M.S., Mizuta, R., Nobre, P., Satoh, M., Scoccimarro, E., Semmler, T., Small, J., von Storch, J.-S., 2016. High resolution model Intercomparison Project (HighResMIP v1.0) for CMIP6.

Geosci. Model Dev. (GMD) 9, 4185–4208. https://doi.org/10.5194/gmd-9-4185-2016, 2016.
Hansen, J., Ruedy, R., Sato, M., Lo, K., 2010. Global surface temperature change. Rev. Geophys. 48 (4) https://doi.org/10.1029/2010RG000345.
Harari, J., França, C.A.S., Camargo, R., 2004. Variabilidade de longo termo de componentes de marés e do nível médio do mar na costa brasileira. Afro-America Gloss News 8 (1), 1–12.
Hersbach, H., Bell, B., Berrisford, P., Hirahara, S., Horányi, A., Muñoz-Sabater, J., et al., 2020. The ERA5 global reanalysis. Q. J. R. Meteorol. Soc. 146 (730), 1999–2049. https://doi.org/10.1002/qj.3803.
Horita, F.E., de Albuquerque, J.P., Degrossi, L.C., Mendiondo, E.M., Ueyama, J., 2015. Development of a spatial decision support system for flood risk management in Brazil that combines volunteered geographic information with wireless sensor networks. Comput. Geosci. 80, 84–94. https://doi.org/10.1016/j.cageo.2015.04.001.
Huang, B., Thorne, P.W., Banzon, V.F., Boyer, T., Chepurin, G., Lawrimore, J.H., Menne, M.J., Smith, T.M., Vose, R.S., Zhang, H., 2017. Extended Reconstructed Sea Surface temperature, version 5 (ERSSTv5): upgrades, validations, and intercomparisons. J. Clim. 30 (20), 8179–8205. https://journals.ametsoc.org/view/journals/clim/30/20/jcli-d-16-0836.1.xml.
Hummell, B.M., Cutter, S.L., Emrich, C.T., 2016. Social vulnerability to natural hazards in Brazil. International Journal of Disaster Risk Science 7 (2), 111–122. https://doi.org/10.1007/s13753-016-0090-9.
IBGE, 2010. IBGE Censo 2010. Brasília, DF. Brasil. https://censo2010.ibge.gov.br/painel/?nivel=mn.
IBGE, 2018. Populações em Área de Risco no Brasil. Brasília, DF. Brasil. https://biblioteca.ibge.gov.br/visualizacao/livros/liv101589.pdf.
IBGE, 2020. Estimativas de População de Recife. https://sidra.ibge.gov.br/pesquisa/estimapop/tabelas. (Accessed 25 June 2022).
Jones, N., 2022. Rare'triple'La Niña climate event looks likely-what does the future hold? Nature. https://doi.org/10.1038/d41586-022-01668-1.
Kakinuma, K., Puma, M.J., Hirabayashi, Y., Tanoue, M., Baptista, E.A., Kanae, S., 2020. Flood-induced population displacements in the world. Environ. Res. Lett. 15 (12), 124029.
Koster, M., 2020. An ethnographic perspective on urban planning in Brazil: temporality, diversity and critical urban theory. Int. J. Urban Reg. Res. 44 (2), 185–199. https://doi.org/10.1111/1468-2427.12765.
Kouadio, Y.K., Servain, J., Machado, L.A.T., Lentini, C.A.D., 2012. Heavy rainfall episodes in the Eastern Northeast Brazil linked to large-scale ocean-atmosphere conditions in the tropical Atlantic. Adv. Meteorol. 1–16. https://doi.org/10.1155/2012/369567, 2012.
Lemos, M.C., Lo, Y.J., Nelson, D.R., Eakin, H., Bedran-Martins, A.M., 2016. Linking development to climate adaptation: leveraging generic and specific capacities to reduce vulnerability to drought in NE Brazil. Global Environ. Change 39, 170–179.
Lenssen, N., Schmidt, G., Hansen, J., Menne, M., Persin, A., Ruedy, R., Zyss, D., 2019. Improvements in the GISTEMP uncertainty model. J. Geophys. Res. Atmos. 124 (12), 6307–6326. https://doi.org/10.1029/2018JD029522.
Li, S., Otto, F.E., 2022. The role of human-induced climate change in heavy rainfall events such as the one associated with Typhoon Hagibis. Climatic Change 172 (1–2), 7. https://doi.org/10.1007/s10584-022-03344-9.
Lins, E.A.M., de Oliveira, E.S., de Oliveira, P.E.S., de Oliveira, J.T.R., 2020. Mapping of risks and dangers of mass movements in hills of the city of recife, pernambuco, Brazil. International Journal of Development Research 10 (7), 38178–38186. https://doi.org/10.37118/ijdr.19515.07.2020.
Liu, C., Zipser, E.J., 2009. "Warm rain" in the tropics: seasonal and regional distributions based on 9 yr of TRMM data. J. Clim. 22 (3), 767–779. https://doi.org/10.1175/2008JCLI2641.1.
Magalhães, A.R., 1996. Adapting to climate variations in developing regions: a planning framework. In: Adapting to Climate Change. Springer, New York, NY. https://doi.org/10.1007/978-1-4613-8471-7_5 et al.
Mansur, A.V., Brondizio, E.S., Roy, S., de Miranda Araújo Soares, P.P., Newton, A., 2018. Adapting to urban challenges in the Amazon: flood risk and infrastructure deficiencies in Belém, Brazil. Reg. Environ. Change 18 (5), 1411–1426. https://doi.org/10.1007/s10113-017-1269-3.
Marchezini, V., Londe, L.D.R., Bernardes, T., Conceiçao, R.S.D., Santos, E.V., Saito, S.M., et al., 2017. Sistema de alerta de risco de desastres no Brasil: desafios à redução da vulnerabilidade institucional. Reduction of vulnerability to disasters: from knowledge to action. São Carlos: Rima Editora 1, 287–310.
Marengo, Jose A., Torres, Roger Rodrigues, Alves, Lincoln Muniz, 2017. Drought in Northeast Brazil—past, present, and future. Theor. Appl. Climatol. 129 (3), 1189–1200. https://doi.org/10.1007/s00704-016-1840-8.
Marengo, J.A., et al., 2019. Increase risk of drought in the semiarid lands of Northeast Brazil due to regional warming above 4 °C. In: Nobre, C., Marengo, J., Soares, W. (Eds.), Climate Change Risks in Brazil. Springer, Cham. https://doi.org/10.1007/978-3-319-92881-4_7.
Marengo, J.A., Galdos, M.V., Challinor, A., Cunha, A.P., Marin, F.R., Vianna, M.D.S., et al., 2021. Drought in Northeast Brazil: a review of agricultural and policy adaptation options for food security. Climate Resilience and Sustainability 1 (1), e17.
Marengo, J.A., Alcantara, E., Cunha, A.P., Seluchi, M., Nobre, C.A., Dolif, G., et al., 2023. Flash floods and landslides in the city of Recife, Northeast Brazil after heavy rain on May 25–28, 2022: causes, impacts, and disaster preparedness. Weather Clim. Extrem. 39, 100545.
Martins, Eduardo SPR., Caio, A.S., Coelho, C.A.S., Haarsma, R., Otto, Friederike EL., King, A.D., Van Oldenborgh, G.J., Kew, S., Sjoukje, P., Vasconcelos Jr, F.C., Cullen, Heidi., 2017. A multimethod attribution analysis of the prolonged northeast Brazil hydrometeorological drought (2012-16). Explaining Extreme Events of 2016 from a Climate Perspective. Special Supplement to the Bulletin of the American Meteorological Society.
MDR. Ministério do Desenvolvimento Regional, 2022. Comitiva Federal irá a Pernambuco neste domingo disponibilizar apoio para regiões afetadas pelas fortes chuvas. https://www.gov.br/mdr/pt-br/noticias/comitiva-federal-ira-a-pernambuco-neste-domingo-disponibilizar-apoio-para-regioes-afetadas-pelas-fortes-chuvas.
Neves, Danielson Jorge Delgado, Alcântara, Clênia Rodrigues, Pereira de Souza, Enio, 2016. Case study of an easterly wave disturbance over Rio Grande do Norte state-Brazil. Revista Brasileira de Meteorologia 31, 490–505.
Oliveira, R.G.D., Cunha, A.P.D., Gadelha, A.G.D.S., Carpio, C.G., Oliveira, R.B.D., Corrêa, R.M., 2020. Racial inequalities and death on the horizon: COVID-19 and structural racism. Cad. Saúde Pública 36. https://doi.org/10.1590/0102-311X00150120.
Philip, S., Kew, S., van Oldenborgh, G.J., Otto, F., Vautard, R., van der Wiel, K., et al., 2020. A protocol for probabilistic extreme event attribution analyses. Adv. Stat. Clim. Meteorol. Oceanogr. 6, 177–203. https://doi.org/10.5194/ascmo-6-177-2020.
Ramos, R.P.L., 1975. Precipitation characteristics in the Northeast Brazil dry region. J. Geophys. Res. 80 (12), 1665–1678. https://doi.org/10.1029/JC080i012p01665, 1975.
Rasch, R.J., 2016. Assessing urban vulnerability to flood hazard in Brazilian municipalities. Environ. Urbanization 28 (1), 145–168. https://doi.org/10.1177/0956247815620961.
Rasch, R., 2017. Income inequality and urban vulnerability to flood hazard in Brazil. Soc. Sci. Q. 98 (1), 299–325. https://doi.org/10.1111/ssqu.12274.
Rayner, N.A.A., Parker, D.E., Horton, E.B., Folland, C.K., Alexander, L.V., Rowell, D.P., et al., 2003. Global analyses of sea surface temperature, sea ice, and night marine air temperature since the late nineteenth century. J. Geophys. Res. Atmos. 108 (D14) https://doi.org/10.1029/2002JD002670.
Relief web, 2010. Brazil: Floods - June 2010. ReliefWeb. https://reliefweb.int/disaster/fl-2010-000120-bra.
Ribot, Jesse C., Najam, Adil, Watson, Gabrielle, 1996. Climate variation, vulnerability and sustainable development in the semi-arid tropics. In: Climate Variability, Climate Change and Social Vulnerability in the Semi-arid Tropics. Cambridge University Press, Cambridge, UK. https://doi.org/10.1017/CBO9780511608308.
Rodrigues, D.T., Gonçalves, W.A., Spyrides, M.H.C., Santos e Silva, C.M., de Souza, D.O., 2020. Spatial distribution of the level of return of extreme precipitation events in Northeast Brazil. Int. J. Climatol. 40 (12), 5098–5113. https://doi.org/10.1002/joc.6507.
Rodrigues, N.M., Rodrigues, C.E.F., Rodrigues, C.R., 2022. A falta de drenagem urbana nas cidades brasileiras. Research, Society and Development 11 (6). https://doi.org/10.33448/rsd-v11i6.29652.
Rozante, J.R., Moreira, D.S., Gonçalves, L.G.G., Vila, D.A., 2010. Combining TRMM and surface observations of precipitation: technique and validation over South America. Weather Forecast. 25, 885–894. https://doi.org/10.1175/2010WAF2222325.1.
Rudorff, C., Sparrow, S., Guedes, M.R.G., Tett, S.F.B., Brêda, J.P.L.F., Cunningham, C., Ribeiro, F.N.D., Palharini, R.S.A., Lott, F.C., 2021. Event attribution of Parnaíba river floods in northeastern Brazil. Climate Resil Sustain 1, e16. https://doi.org/10.1002/cli2.16.
Schneider, Udo, Becker, Andreas, Finger, Peter, Elke, Rustemeier, Ziese, Markus, 2020. GPCC Monitoring Product: Near Real-Time Monthly Land-Surface Precipitation from Rain-Gauges Based on SYNOP and CLIMAT Data. https://doi.org/10.5676/DWD_GPCC/MP_M_V2020_100, 10.5676/DWD_GPCC/MP_M_V2020_100.
Seneviratne, S.I., Zhang, X., Adnan, M., Badi, W., Dereczynski, C., Di Luca, A., Ghosh, S., Iskandar, I., Kossin, J., Lewis, S., Otto, F., Pinto, I., Satoh, M., Vicente-Serrano, S.M., Wehner, M., Zhou, B., 2021. Weather and climate extreme events in a changing climate. In: Masson-Delmotte, V., Zhai, P., Pirani, A., Connors, S.L., Péan, C., Berger, S., Caud, N., Chen, Y., Goldfarb, L., Gomis, M.I., Huang, M., Leitzell, K., Lonnoy, E., Matthews, J.B.R., Maycock, T.K., Waterfield, T., Yelekçi, O., Yu, R., hZhou, B. (Eds.), Climate Change 2021: the Physical Science Basis. Contribution of Working Group I to the Sixth Assessment Report of the Intergovernmental Panel on Climate Change. Cambridge University Press, Cambridge, United Kingdom and New York, NY, USA, pp. 1513–1766. https://doi.org/10.1017/9781009157896.013.
Silva, T.L. do V., de Souza Guedes, R.V., 2012. Análise do Comportamento Atmosférico em Situação de Seca: Uma Abordagem Operacional para Pernambuco (Analysis of Atmospheric Behavior Under Drought Condition: An Operational Approach to Pernambuco). Revista Brasileira de Geografia Física 5 (4), 937–950. Retrieved from. https://periodicos.ufpe.br/revistas/rbgfe/article/download/232880/26871.
Silva, M.A.B.D., Silva, S.R.D., Cabral, J.J.D.S.P., 2017. Compensatory Alternatives for Flooding Control in Urban Areas with Tidal Influence in Recife-PE, vol. 22. RBRH.
Silva, T.L. do V., Veleda, D., Araujo, M., Tyaquiçã, P., 2018. Ocean-atmosphere feedback during extreme rainfall events in eastern Northeast Brazil. J. Appl. Meteorol. Climatol. 57 (5), 1211–1229. https://doi.org/10.1175/JAMC-D-17-0232.1.
Silva, Bruce Francisco Pontes, Rocha, Rosmeri Porfírio da, Gomes, Helber Barros, 2020. Easterly wave disturbances activity over the Eastern Northeast Brazil during 2006-2010 rainy seasons. Revista Científica Foz 3 (2), 30-30.
Souza Leao, E.B., Andrade, J.C.S., Nascimento, L.F., 2021. Recife: a climate action profile. Cities 116, 103270. https://doi.org/10.1016/j.cities.2021.103270.
Taylor, K.E., Stouffer, R.J., Meehl, G.A., 2012. An overview of CMIP5 and the experiment design. Bull. Am. Meteorol. Soc. 93 (4), 485–498. https://doi.org/10.1175/BAMS-D-11-00094.1.
Torres, R.R., Ferreira, N.J., 2011. Case studies of easterly wave disturbances over Northeast Brazil using the eta model. Weather Forecast. 26 (2), 225–235. https://doi.org/10.1175/2010WAF2222425.1.
Vale Silva, T.L., Lopes, Z., Ferreira, R., Guedes, R., Pereira, R., Prestrelo, F., Dias, H., 2023. Previsão de extremos de chuva em Pernambuco: os eventos de maio de 2022. Revista Brasileira de Geografia Física 16 (1), 646–671.

Van Oldenborgh, G.J., van der Wiel, K., Kew, S., Philip, S., Otto, F., Vautard, R., et al., 2021. Pathways and pitfalls in extreme event attribution. Climatic Change 166 (1), 13. https://doi.org/10.1007/s10584-021-03071-7.

Vecchi, G.A., Delworth, T., Gudgel, R., Kapnick, S., Rosati, A., Wittenberg, A.T., et al., 2014. On the seasonal forecasting of regional tropical cyclone activity. J. Clim. 27 (21), 7994–8016. https://doi.org/10.1175/JCLI-D-14-00158.1.

Waliser, D.E., Jiang, X., 2015. Tropical meteorology: Intertropical convergence zone. In: North, G.R., Pyle, J., Zhang, F. (Eds.), Encyclopedia of Atmospheric Sciences, second ed. Elsevier, pp. 121–131.

World Bank, 2012a. Avaliação de perdas e danos: inundações bruscas em Pernambuco Junho de 2010. Brasília,DF. https://antigo.mdr.gov.br/images/stories/ArquivosDefesaCivil/ArquivosPDF/publicacoes/Inundaes-Bruscas-em-Pernambuco.pdf.

World Bank, 2012b. Avaliação de perdas e danos: inundações bruscas em Alagoas. Junho de 2010. Brasília,DF. https://antigo.mdr.gov.br/images/stories/ArquivosDefesaCivil/ArquivosPDF/publicacoes/Inundaes-Bruscas-em-Alagoas.pdf.

World Bank, 2020. Relatório de danos Materiais e Prejuízos decorrentes de Desastres Naturais do Brasil de 1995 a 2019. Brasília, DF. https://www.gov.br/mdr/pt-br/centrais-de-conteudo/publicacoes/protecao-e-defesa-civil-sedec/danos_e_prejuizos_versao_em_revisao.pdf.

Yang, W., Hsieh, T.L., Vecchi, G.A., 2021. Hurricane annual cycle controlled by both seeds and genesis probability. Proc. Natl. Acad. Sci. USA 118 (41), e2108397118. https://doi.org/10.1073/pnas.2108397118.

Ziese, Markus, Becker, Andreas, Finger, Peter, Meyer-Christoffer, Anja, Rudolf, Bruno, Schneider, Udo, 2011. GPCC first guess product at 1.0°: near real-time first guess monthly land-surface precipitation from rain-gauges based on SYNOP data. https://doi.org/10.5676/DWD_GPCC/FG_M_100.